*Effect of YY1 and E2F1 overexpression on the transcription activity of p73*

Next, to assess the effect of YY1 overexpression and to confirm that of E2F1, a well-known p73 regulator, on p73 promoter activity, we generated a YY1-expression vector (pcDNA3-YY1) and an E2F1 expression vector (pcEF9-Flag-E2F1), and confirmed their expressions by Western blot analysis (Fig. 2A). Furthermore, the p53-inhibition activity of exogenous YY1 was also confirmed by p21 luciferase/reporter (Supplemental Fig. 2). Then, a different dose of the pcDNA3-YY1 was co-transfected into U2ff S cells together with the two p73 reporters (Fig. 2B). The results were in agreement with those of knockdown experiments, as overexpression of YY1 led to the activation of the p73 promoter in a plasmid-dose dependent manner. Similar results were also obtained from Saff S2 cells, a p53 deficient human osteocarcinoma cell line (Fig. 2C), indicating that the YY1-induced p73 transcriptional activity is independent on p53 status. ff n the other hand, overexpressing E2F1 by co-transfecting E2F1 expression vector with the p73 promoter (−4052/+438)/reporter (Fig. 2D) or the p73 promoter (−857/+71)/reporter (Supplemental Fig. 3) resulted in the significant induction of both p73 reporters' activities, as shown previously [13]. Moreover, YY1 overexpression in U2ff S cells resulted in the increase of endogenous p73 mRNA (Fig. 2E), similar with the effect of doxorubicin (Fig. 2F), which has been known to induce p73 activity via E2F1.

Collectively, the results from the knockdown and overexpression experiments for YY1 clearly identified the previously unsuspected role of YY1, i.e., the possibility that tumor activator gene YY1 up-regulates the transcriptional activity of p73. Recently, other evidences showed that spontaneous tumor formation did not develop in p73-null mice, and infrequent p73 mutations or overexpression of p73 protein was seen in a variety of tumors [17]; raising

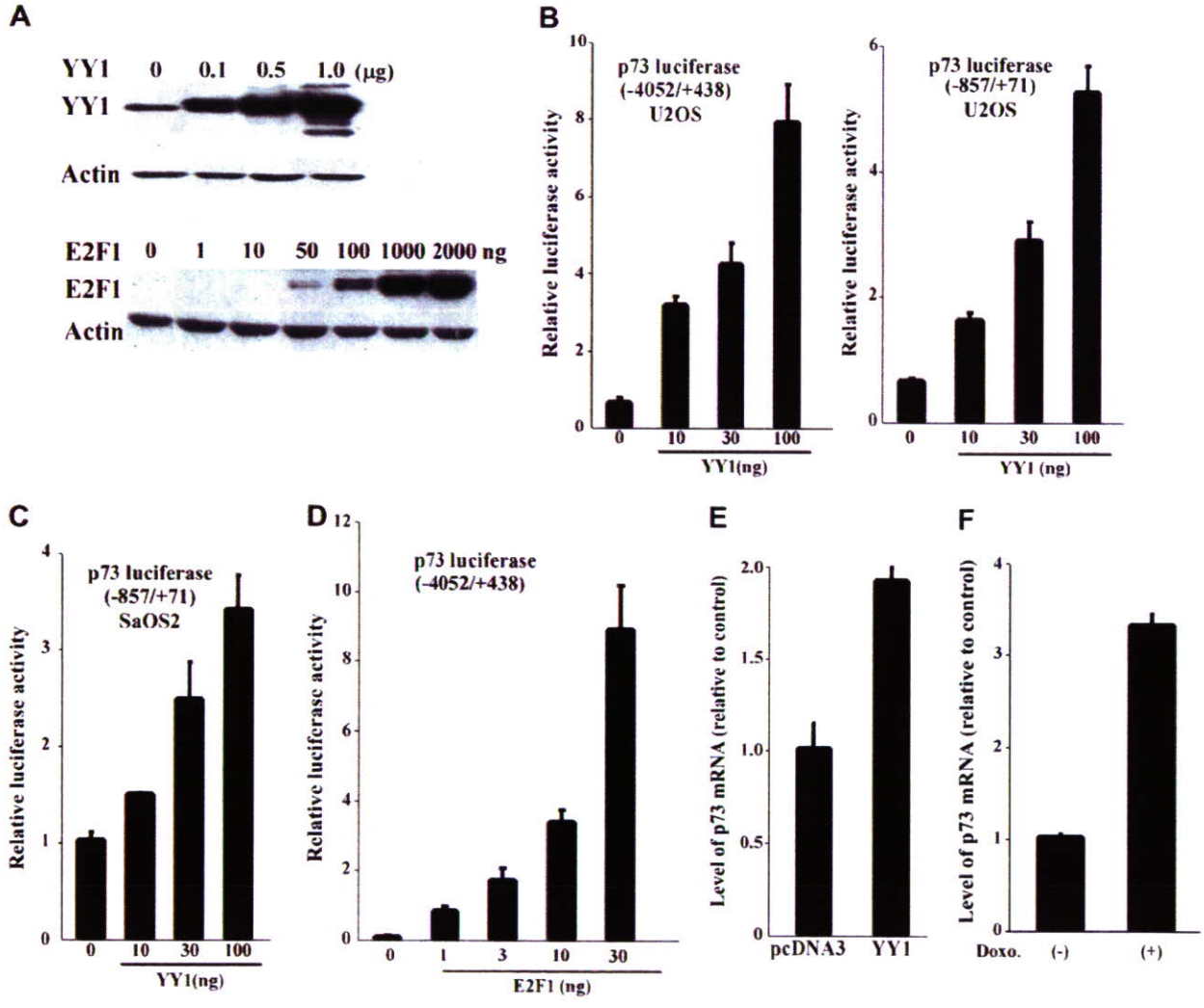


Fig. 2. The induction of p73 promoter activity by YY1 and E2F1. (A) Western blotting analysis of YY1 (upper panel) and E2F1 (lower panel) in HCT116 cells transfected with pcDNA3-YY1 or pcEF9-Flag-E2F1. (B) The effect of YY1 on the activities of p73 luciferase (−4052/+438)/reporter (left) or p73 luciferase (−857/+71)/reporter (right) in U2ff S cells, determined by dual luciferase assay 48 h after transfection. (C) The effect of YY1 on the activities of p73 luciferase (−857/+71)/reporter in Saff S2 cells. (D) The effect of E2F1 on the activities of the p73 luciferase (−4052/+438)/reporter in HCT116 cells. (E) Expression of p73 mRNA in U2ff S cells transfected with pcDNA3-YY1, determined by real-time RT-ffCR analysis 12 h after transfection. (F) Expression of p73 mRNA in U2ff S cells treated with doxorubicin (2 μM), determined by real-time RT-ffCR analysis 24 h after treatment.

the question of the function of p73 as a tumor suppressor gene. A very recent work by Vikhanskaya et al. provided a potential answer to this question [12]. They found that p73 could promote cellular growth in a synergistic manner with the proto-oncogene c-Jun through Affi1 up-regulation, thus, p73 could positively act for tumorigenesis. ff ur results were consistent with their results. Moreover, it has also been reported that Yin Yang 1 is essential for oligodendrocyte progenitor differentiation and B-cell development [18,19]. Thus, our findings might also provide an important clue for unveiling molecular functions and mechanisms of YY1 and p73 pathway in neural differentiation and development. Therefore, we next addressed how YY1 regulates p73 gene transcription, specifically, whether there is a relationship between YY1 and E2F1 in regulating the transcriptional activity of p73.

*The synergistic effect of YY1 and E2F1 on p73 transactivation*

To examine whether there is cooperative regulation of p73 promoter activity by E2F1 and YY1, we performed co-transfection experiments using the p73 promoter (−4052/+438)/reporter, pcDNA3-YY1 and pEF9-E2F1 vectors. The U2ff S cells co-transfected with both E2F1-expression and YY1-expression vectors showed a signification enhancement in the activity of p73 promoter compared to cells transfected with either of the vectors alone (Fig. 3A). Furthermore, in experiments with serial doses of YY1-expression vector under the constant presence of pEF9-E2F1, we found that in the presence of E2F1, the activity of p73 promoter increased in a dose-dependent manner with increasing amount of pcDNA-YY1 vector (Fig. 3B). These results demonstrated that YY1 could induce the transcriptional activity of p73 in a synergistic fashion with E2F1.

ffreviously, Schlisio et al. reported that E2F2 and E2F3, the members of E2F family, could interact with YY1 through mediation of the RYBffi protein on the cdc6 promoter; they suggested that the interaction of E2Fs family with YY1 might determine the specificity of E2F2/E2F3 or E2F1 for different promoters [20]. In this study, we observed considerable cooperative transcriptional activation between E2F1 and YY1 on the p73 promoter. However, this functional interaction between YY1 and E2F1 might be not general, as the overexpression of YY1 did not show any significant activation of other well-defined E2F1-dependent promoters tested (DNMT1 and DHFR, data not shown), suggesting that the promoter specificity of E2F1 and E2F2/E2F3 is not simply determined by the

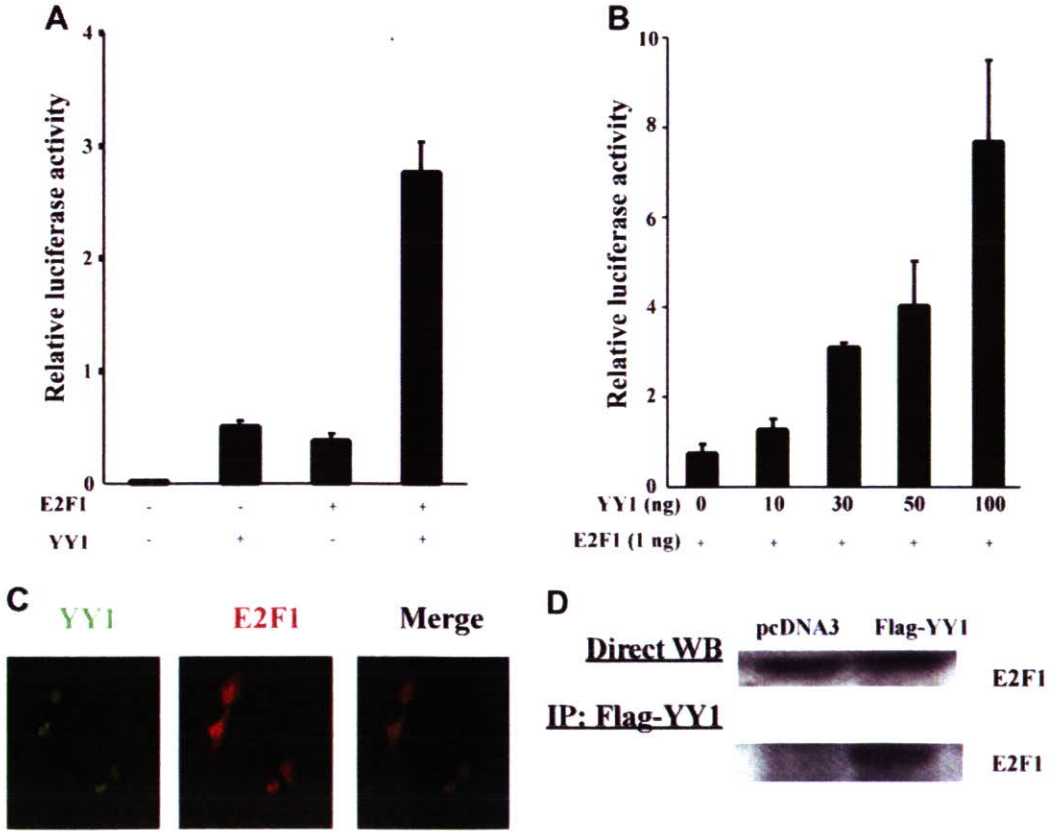


Fig. 3. The synergistic effect of YY1 and E2F1 on the transcriptional activation p73. (A) The activity of p73 luciferase (−4052/+438)/reporter in U2ff S cells transfected with mock vector, pcDNA3-Flag-YY1 (50 ng), pcEF9-Flag-E2F1 (1 ng), or both pcDNA3-YY1 (50 ng) and pcEF9-Flag-E2F1 (1 ng). Dual luciferase assay was performed 48 h after transfection. (B) The activity of p73 luciferase (−4052/+438)/reporter in U2ff S cells transfected with the indicated amounts of pcDNA3-YY1 and the constant amount of pcEF9-Flag-E2F1 (1 ng). (C) Immunofluorescence staining of YY1 and E2F1 in U2ff S cells. (D) Co-immunoprecipitation of E2F1 and YY1 in HEK293T cells. Cells were lysed and pulled-down with anti-Flag antibody.

interaction with YY1, but might be determined by other undefined factors interacting with E2Fs and/or the epigenetic status of the promoters.

*Co-localization and interaction between YY1 and E2F1*

To understand the cellular and molecular mechanisms of the synergistic effects between YY1 and E2F1 on p73 promoter activation, we first examined the subcellular localization of YY1 and E2F1. As shown in Fig. 3C, YY1 was largely colocalized with E2F1 in the nucleus. Next, we examined the physical interactions between YY1 and E2F1 by performing co-immunoprecipitation experiments. The results showed that E2F1 immunoprecipitated in cells transfected with the Flag-YY1-expression vector, whereas no band was detected in cells transfected with the control vector (Fig. 3D). These observations demonstrated the direct physical association between YY1 and E2F1.

*Role of YY1 in DNA damage-induced transcriptional activity of p73 promoter*

As reported previously, the p73 promoter was activated E2F1-dependently by doxorubicin, a DNA damaging agent [13]. Therefore, we examined whether YY1 contributed to doxorubicin-induced p73 transcriptional activation. YY1-silenced cells showed significant reduction in the activation of the p73 promoter induced by doxorubicin (Fig. 4A, B), which was similar to that of E2F1-silencing cells.

Furthermore, p73 promoter activation by doxorubicin treatment has been reported to be critically dependent on

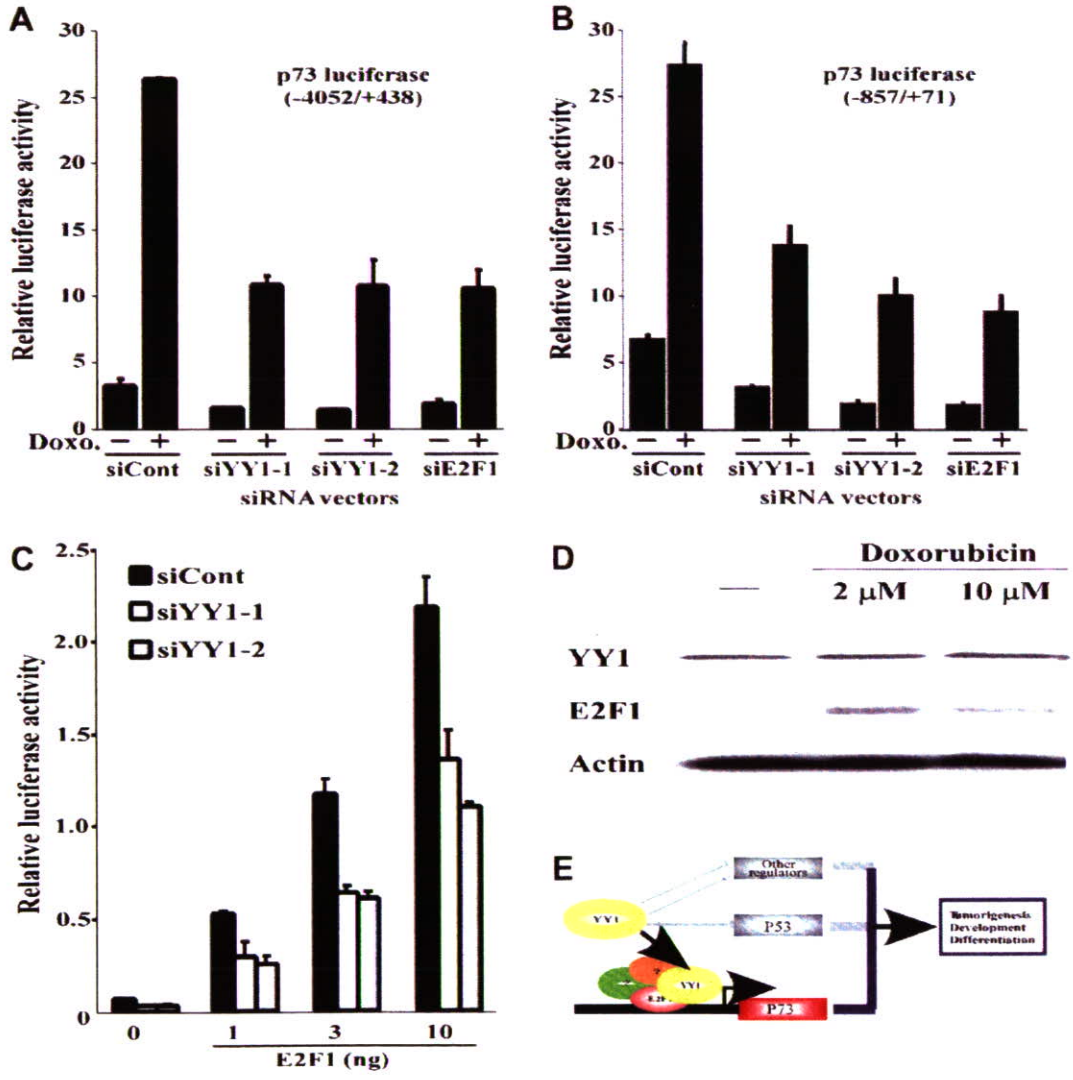


Fig. 4. Involvement of YY1 in transcriptional activation of p73 induced by doxorubicin. (A, B) The activity of p73 promoter in the YY1-silenced U2ff S cells under doxorubicin treatment. siYY1-1, siYY1-2 or siE2F1 vectors-transfected U2ff S cells were co-transfected with p73 luciferase (−4052/+438)/reporter (A) or (−857/+71)/reporter (B) and pRL-SV40. Twenty-four hours after transfection, U2ff S cells were untreated or treated with doxorubicin (2 μM), and 24 h later, dual luciferase assay was performed. (C) The effect of YY1-silencing on p73 promoter activity induced by E2F1 in U2ff S cells. The indicated siRNA vectors-transfected U2ff S cells were co-transfected with p73 luciferase (−4052/+438)/reporter and increasing amount of pcEF9-Flag-E2F1. (D) Western blot analysis of E2F1 and YY1 in HCT116 cells treated by doxorubicin. (E) A model of the co-regulation of YY1 and E2F1 on p73.

E2F1 [13]. Based on the interaction of E2F1 and YY1, we next tested whether p73 promoter activation by E2F1 overexpression also showed the YY1 dependency. The YY1-knocked down cells were co-transfected with serial doses of E2F1-expression vectors and the p73 reporter vector. As shown in Fig. 4C, in YY1-silenced cells, the p73 promoter activation induced by E2F1 was significantly reduced, which was a comparable suppressive effect as that of doxorubicin-treated cells, suggesting that the YY1 signal might be constitutive during doxorubicin treatment. Together with the results of Western blot analysis (Fig. 4D), which revealed that only endogenous E2F1, not YY1 expression was induced by doxorubicin treatment, these data indicated that cooperative action between the constitutive YY1 and the inducible E2F1 contributes to the activation of the p73 promoter under the treatment with doxorubicin. Furthermore, YY1-silencing did not affect the expression of endogenous E2F1 (Fig. 1A), which also strongly suggested that YY1 induces the transcriptional activity of p73 by cooperation with E2F1, not via increasing E2F1.

Taken together, our results uncovered a novel function of YY1 on E2F1-mediated p73 regulation. We summarized the model in Fig. 4E. The fact that YY1 affects p53 family members opened up an attractive possibility that needs further investigation, that is, YY1 might function as a key integrator or modulator of various pathways in the network that includes p53 family members and regulators concerned with cancer progression, development and differentiation.

## Acknowledgments

We thank ffrof. Massimo Levrero at the University of Rome 'La Sapienza' for kindly providing the p73 reporter vector. This work was partially supported by a grant from the 21st Century CffE ffrogram, School of Medicine, The University of Tokyo, and a grant for Research on ffsychiatric and Neurological Diseases and Mental Health, the Ministry of Health, Labour and Welfare of Japan.

## Appendix A. Supplementary data

Supplementary data associated with this article can be found, in the online version, at doi:10.1016/j.bbrc.2007.10.145.

## References

[1] Y. Shi, E. Seto, L.S. Chang, T. Shenk, Transcriptional repression by YY1, a human GLI-Kruppel-related protein, and relief of repression by adenovirus E1A protein, Cell 67 (1991) 377–388.

[2] K. ffark, M.L. Atchison, Isolation of a candidate repressor/activator, NF-E1 (YY-1, delta), that binds to the immunoglobulin kappa 3' enhancer and the immunoglobulin heavy-chain mu E1 site, ffroc. Natl. Acad. Sci. USA 88 (1991) 9804–9808.

[3] S. Gordon, G. Akopyan, H. Garban, B. Bonavida, Transcription factor YY1: structure, function, and therapeutic implications in cancer biology, ff ncogene 25 (2006) 1125–1142.

[4] M.E. Donohoe, X. Zhang, L. McGinnis, J. Biggers, E. Li, Y. Shi, Targeted disruption of mouse Yin Yang 1 transcription factor results in peri-implantation lethality, Mol. Cell. Biol. 19 (1999) 7237–7244.

[5] B. Affar el, F. Gay, Y. Shi, H. Liu, M. Huarte, S. Wu, T. Collins, E. Li, Essential dosage-dependent functions of the transcription factor yin yang 1 in late embryonic development and cell cycle progression, Mol. Cell. Biol. 26 (2006) 3565–3581.

[6] G. Sui, B. Affar el, Y. Shi, C. Brignone, N.R. Wall, ffi Yin, M. Donohoe, M.ffi Luke, D. Calvo, S.R. Grossman, Yin Yang 1 is a negative regulator of p53, Cell 117 (2004) 859–872.

[7] R. Agami, G. Blandino, M. ff ren, Y. Shaul, Interaction of c-Abl and p73alpha and their collaboration to induce apoptosis, Nature 399 (1999) 809–813.

[8] C.A. Jost, M.C. Marin, W.G. Kaelin Jr., p73 is a simian [correction of human] p53-related protein that can induce apoptosis, Nature 389 (1997) 191–194.

[9] G. Melino, F. Bernassola, M. Ranalli, K. Yee, W.X. Zong, M. Corazzari, R.A. Knight, D.R. Green, C. Thompson, K.H. Vousden, p73 Induces apoptosis via ffUMA transactivation and Bax mitochondrial translocation, J. Biol. Chem. 279 (2004) 8076–8083.

[10] G. Meyer, C.G. ffrez-Garcia, H. Abraham, D. Caput, Expression of p73 and Reelin in the developing human cortex, J. Neurosci. 22 (2002) 4973–4986.

[11] T. ff zaki, M. Hosoda, K. Miyazaki, S. Hayashi, K. Watanabe, T. Nakagawa, A. Nakagawara, Functional implication of p73 protein stability in neuronal cell survival and death, Cancer Lett. 228 (2005) 29–35.

[12] F. Vikhanskaya, W.H. Toh, I. Dulloo, Q. Wu, L. Boominathan, H.H. Ng, K.H. Vousden, K. Sabapathy, p73 supports cellular growth through c-Jun-dependent Affi1 transactivation, Nat. Cell Biol. 9 (2007) 698–705.

[13] N. ffediconi, A. Ianari, A. Costanzo, L. Belloni, R. Gallo, L. Cimino, A. ffbrcellini, I. Screpanti, C. Balsano, E. Alesse, A. Gulino, M. Levrero, Differential regulation of E2F1 apoptotic target genes in response to DNA damage, Nat. Cell Biol. 5 (2003) 552–558.

[14] M. Miyagishi, R. Fujii, M. Hatta, E. Yoshida, N. Araya, A. Nagafuchi, S. Ishihara, T. Nakajima, A. Fukamizu, Regulation of Lef-mediated transcription and p53-dependent pathway by associating beta-catenin with CBfff/p300, J. Biol. Chem. 275 (2000) 35170–35175.

[15] M. Miyagishi, K. Taira, U6 promoter-driven siRNAs with four uridine 3' overhangs efficiently suppress targeted gene expression in mammalian cells, Nat. Biotechnol. 20 (2002) 497–500.

[16] M. Miyagishi, K. Taira, Strategies for generation of a siRNA expression library directed against the human genome, ff ligonucleotides 13 (2003) 325–333.

[17] F. de Nigris, C. Botti, A. de Chiara, R. Rossiello, G. Apice, F. Fazioli, C. Fiorito, V. Sica, C. Napoli, Expression of transcription factor Yin Yang 1 in human osteosarcomas, Eur. J. Cancer 42 (2006) 2420–2424.

[18] Y. He, J. Dupree, J. Wang, J. Sandoval, J. Li, H. Liu, Y. Shi, K.A. Nave, ffi Casaccia-Bonnefil, The transcription factor Yin Yang 1 is essential for oligodendrocyte progenitor differentiation, Neuron 55 (2007) 217–230.

[19] H. Liu, M. Schmidt-Supprian, Y. Shi, E. Hobeika, N. Barteneva, H. Jumaa, R. ffelanda, M. Reth, J. Skok, K. Rajewsky, Yin Yang 1 is a critical regulator of B-cell development, Genes Dev. 21 (2007) 1179–1189.

[20] S. Schlisio, T. Halperin, M. Vidal, J.R. Nevins, Interaction of YY1 with E2Fs, mediated by RYBffi provides a mechanism for specificity of E2F function, EMBff J. 21 (2002) 5775–5786.

OPEN ACCESS Freely available online

PLoS one

# An Excellent Monitoring System for Surface Ubiquitination-Induced Internalization in Mammals

Eiji Goto[1], Mari Mito-Yoshida[1], Mika Uematsu[1], Masami Aoki[1], Yohei Matsuki[1], Mari Ohmura-Hoshino[1], Hak Hotta[2], Makoto Miyagishi[3], Satoshi Ishido[1]*

1 Laboratory for Infectious Immunity, RIKEN Research Center for Allergy and Immunology, Yokohama, Kanagawa, Japan, 2 Department of Pathology and Microbiology, Kobe University Graduate School of Medicine, Kobe, Hyogo, Japan, 3 21st Century COE Program, School of Medicine, The University of Tokyo, Tokyo, Japan

***Background.*** At present, it is difficult to visualize the internalization of surface receptors induced by ubiquitination that is taken place at the plasma membrane in mammals. This problem makes it difficult to reveal molecular basis for ubiquitination-mediated internalization in mammals. ***Methodology / Principle Findings.*** In order to overcome it, we have generated T-REx-c-MIR, a novel mammalian Tet-on B cell line using a constitutively active E3 ubiquitin ligase, c-MIR, and its artificial target molecule. By applying the surface biotinylation method to T-REx-c-MIR, we succeeded to monitor the fate of surface target molecules after initiation of ubiquitination process by doxycycline (Dox)-induced c-MIR expression. Target molecules that pre-existed at the plasma membrane before induction of c-MIR expression were oligo-ubiquitinated and degraded by Dox-induced c-MIR expression. Dox-induced c-MIR expression initiated rapid internalization of surface target molecules, and blockage of the internalization induced the accumulation of the surface target molecules that were newly ubiquitinated by c-MIR. Inhibition of the surface ubiquitination by down-regulating ubiquitin conjugating enzyme E2 impaired the internalization of target molecules. Finally, a complex of c-MIR and target molecule was detected at the plasma membrane. ***Conclusions / Significances.*** These results demonstrate that in T-REx-c-MIR, surface target molecule is ubiquitinated at the plasma membrane and followed by being internalized from the plasma membrane. Thus, T-REx-c-MIR is a useful experimental tool to analyze how surface ubiquitination regulates internalization in mammals.

Citation: Goto E, Mito-Yoshida M, Uematsu M, Aoki M, Matsuki Y, et al (2008) An Excellent Monitoring System for Surface Ubiquitination-Induced Internalization in Mammals. PLoS ONE 3(1): e1490. doi:10.1371/journal.pone.0001490

## INTRODUCTION

Ubiquitination is a well-known post-transcriptional modification in eukaryote. Ubiquitination plays important roles in gene transcription, membrane traffic, and signal transduction [1]. During ubiquitination, a small molecule named ubiquitin, whose MW is 8 kD, is covalently conjugated to the target substrate through two different modes: mono-ubiquitination and poly-ubiquitination. Conjugation with one ubiquitin molecule and with tandem repeated ubiquitin molecules is defined as mono- and poly-ubiquitination, respectively. Among the cases of poly-ubiquitination, conjugation with a few ubiquitin molecules is called oligo-ubiquitination. Ubiquitination is sequentially achieved by the cooperation of three enzymes: ubiquitin activating enzyme (E1), ubiquitin conjugating enzyme (E2), and ubiquitin ligase (E3). Among these enzymes, E3 determines its specific substrate for ubiquitination by binding to the molecule to be ubiquitinated [1].

Classically, ubiquitination is recognized as a signal for degradation at the proteasome [2]. In the case of incorrectly folded proteins, these undesired proteins undergo K48-linked chain ubiquitination and are degraded at the proteasome [2]. These systems are required to maintain the quality of functional proteins. Several receptors that induce signals required for development and homeostasis are ubiquitinated. Unlike incorrectly folded proteins, these ubiquitinated receptors are degraded in the lysosome [3,4]. This ubiquitination-mediated lysosomal degradation functions as a negative feedback signal and is required to maintain homeostasis [5]. Indeed, several mutations that disrupt the ubiquitination activity of c-Cbl, an E3 for the EGF receptor, have been found in cancer [6]. Cancer cells carrying a mutation in the RING domain of c-Cbl cannot down-regulate signaling from the EGF receptor. Also, the mutant form of growth factor receptor that cannot associate with a responsible E3 induces sustained signals and promotes hematopoietic malignancy (e.g., leukemia) [7,8]. Thus, the investigation of ubiquitination-mediated membrane trafficking is important to understand how homeostasis is regulated in vivo.

Among the many steps involved in the ubiquitination-mediated membrane trafficking, internalization from the plasma membrane is the first and most critical step for the desensitization of signaling derived from several receptors [9]. Using yeast as an experimental model, the molecular mechanisms underlying ubiquitination-mediated membrane trafficking were intensively investigated [3,9,10]. It has been clearly demonstrated that surface ubiquitination initiates the internalization of plasma membrane proteins including receptors for G-proteins, by analyzing several mutants of yeast [3]. However in mammals, it is difficult to analyze the relationship between surface ubiquitination and internalization of target surface molecules as there are no suitable experimental models in mammals.

In order to overcome this problem, we have established a novel Tet-on B cell line named T-REx-c-MIR by employing a constitutively active ubiquitin ligase, c-MIR [11–14]. As we have reported before, doxycycline (Dox)-induced c-MIR expression leads

**Academic Editor:** Howard Riezman, University of Geneva, Switzerland

**Received** August 30, 2007; **Accepted** December 30, 2007; **Published** January 30, 2008



**Funding:** This work was supported by a Grant-in-Aid for Scientific Research from the Ministry of Education, Science, Sports, and Culture (MEXT) of Japan and by the Japan Society for the Promotion of Science (JSPS).

**Competing Interests:** The authors have declared that no competing interests exist.

* **To whom correspondence should be addressed.** E-mail: ishido@rcai.riken.jp

to ubiquitination and internalization of target molecules (e.g., MHC class II (MHC II) and B7-2). By applying the surface biotinylation method to this cell line, we succeeded in clearly monitoring the fate of surface target molecules after initiation of ubiquitination by Dox-mediated c-MIR expression. Blockage of the internalization with pharmacological reagents induced the accumulation of target surface molecules that were newly ubiquitinated by c-MIR. Inhibition of surface ubiquitination by down-regulating E2 impaired internalization of the target surface molecule. In addition, a complex of c-MIR and target molecule was detected on the plasma membrane. These results demonstrate that in T-REx-c-MIR, surface target molecule is ubiquitinated at the plasma membrane and followed by being internalized from the plasma membrane. Thus, T-REx-c-MIR is a useful experimental tool to analyze how surface ubiquitination regulates internalization in mammals.

## RESULTS

### Generation of T-REx-c-MIR

In order to monitor the surface events initiated by ubiquitination in mammals, we have generated a novel experimental tool, Tet-on B cell line, and named it T-REx-c-MIR. Using this system, we were able to observe specific down-regulation of target molecules by doxycycline (Dox)-induced c-MIR expression. c-MIR was expressed within 2 hr after adding Dox, and this was followed by down-regulation of the surface expression of MHC II and B7-2, which are substrates for c-MIR [11,13] (data not shown, Figure 1B). In contrast, MHC class I (MHC I), which is not a substrate for c-MIR, was not down-regulated (Figure 1B). We examined whether the ubiquitination of endogenous B7-2 molecules is detectable in T-REx-c-MIR. Unfortunately, we could not detect the ubiquitinated form of B7-2 unless these cells were treated with bafilomycin A1 (Figure S1), which has been shown to be a potent inhibitor for c-MIR-induced degradation in our previous work [11]. Therefore, CD8-B7-2-A2, a FLAG-tagged CD8 chimeric target molecule, was expressed in this system to improve visualization of the ubiquitination status of target molecules (Figure 1A). CD8-B7-2-A2 consists of an amino-terminal FLAG-tagged CD8 extracellular domain, a B7-2 transmembrane domain, and a cytoplasmic tail of MHC I, and can be efficiently purified with anti-FLAG M2 beads (Figure 1A). As shown in Figure 1B, CD8-B7-2-A2, but not CD8-A2, which consists of an HLA-A2 transmembrane domain instead of the B7-2 transmembrane domain, was efficiently down-regulated, demonstrating that CD8-B7-2-A2 can be utilized as a substrate for c-MIR in this system.

First, we examined whether surface CD8-B7-2-A2 is degraded by Dox-induced c-MIR. Surface molecules of T-REx-c-MIR were biotinylated with a membrane-impermeable reagent first, and biotinylated T-REx-c-MIR was incubated at 37°C in the presence of Dox for the indicated times. At the end of each incubation, biotinylated proteins including CD8-B7-2-A2 were purified with streptavidin beads and subjected to western blot analysis with anti-FLAG M2 antibody (Ab). As shown in Figure 1C, after induction for 6–8 hr, the amount of surface CD8-B7-2-A2 was significantly decreased compared with that without induction.

Next, the status of ubiquitination of CD8-B7-2-A2 was analyzed by purification from whole cell lysate. To prevent contamination with CD8-B7-2-A2-associated molecules, CD8-B7-2-A2 was purified from protein samples boiled in 1% SDS-containing RIPA buffer. Purified CD8-B7-2-A2 was analyzed with anti-FLAG and anti-ubiquitin Abs. As marked with asterisks in Figure 1D, additional bands recognizable with both anti-FLAG and anti-ubiquitin Abs appeared when Dox was added, confirming that CD8-B7-2-A2 itself was ubiquitinated by c-MIR in T-REx-c-MIR. Furthermore, we investigated whether surface CD8-B7-2-A2 is ubiquitinated by Dox-induced c-MIR. After surface molecules including CD8-B7-2-A2 on T-REx-c-MIR were biotinylated with a membrane-impermeable reagent, c-MIR was expressed by adding Dox in biotinylated T-REx-c-MIR. After induction of c-MIR expression, CD8-B7-2-A2 that pre-exists at the plasma membrane before the process of ubiquitination starts was purified by two sequential steps at each indicated time point (see Materials and methods). Purified CD8-B7-2-A2 was subjected to western blot analysis with anti-FLAG and anti-ubiquitin Abs. As shown in Figure 1E, surface CD8-B7-2-A2 was clearly ubiquitinated after incubation with Dox for 4 hr, and ubiquitinated CD8-B7-2-A2 was degraded after incubation for 8 hr (Figure 1E). Without the procedure of surface biotinylation, we could not observe any signals (data not shown).

Lastly, we examined whether CD8-B7-2-A2 is internalized from plasma membrane. After induction with Dox for 6 hr, surface CD8-B7-2-A2 was labeled with FITC-conjugated anti-CD8 Ab, and the trafficking of labeled CD8-B7-2-A2 was examined by fluorescence microscopy. As shown in Figure 1F, labeled CD8-B7-2-A2 molecules were efficiently internalized by adding Dox. These data were confirmed by using FACS-based analysis (Figure 1F). Taken together, these data demonstrate that T-REx-c-MIR is a useful experimental tool to analyze how ubiquitination contributes to the internalization and degradation of target surface molecules.

### Accumulation of ubiquitinated surface CD8 chimera by inhibiting internalization

The experiments performed above revealed that surface CD8-B7-2-A2 is indeed ubiquitinated by the induced c-MIR expression, but did not show that the ubiquitination of surface CD8-B7-2-A2 takes place at the plasma membrane. Therefore, we examined whether ubiquitinated surface CD8 chimera is accumulated by inhibiting internalization. To this end, we examined the ability of several pharmacological reagents to inhibit internalization induced by c-MIR. Among the reagents examined, chlorpromazine and dansylcadaverine, which are inhibitors of clathrin-dependent internalization, significantly inhibited the down-regulation of CD8-B7-2-A2 without inhibiting c-MIR expression induced by Dox (data not shown, Figure 2A). Consistent with this, the internalization of surface CD8 molecules was inhibited by these reagents (Figure 2B). These results suggest that c-MIR induces the internalization of surface CD8-B7-2-A2 in a clathrin-dependent manner.

Based on these results, we employed chlorpromazine for the following experiments. After surface molecules of T-REx-c-MIR were biotinylated, c-MIR was expressed by adding Dox in the presence or absence of chlorpromazine. After incubation of biotinylated T-REx-c-MIR with Dox for 8 hr, surface biotinylated CD8-B7-2-A2 was purified and analyzed as performed in Figure 1E. As shown in Figure 2C, in the presence of chlorpromazine (+CPZ), ubiquitinated form of biotinylated CD8-B7-A2 was clearly detected even by adding Dox (+), demonstrating that the surface CD8-B7-2-A2 that was newly ubiquitinated by c-MIR was accumulated by blockage of internalization. These results demonstrate that the ubiquitination of CD8-B7-2-A2 takes place at the plasma membrane in T-REx-c-MIR.

### Lysine-less target molecules are neither ubiquitinated nor internalized in T-REx-c-MIR

We examined whether non-ubiquitinated surface CD8-B7-2-A2 is less internalized in T-REx-c-MIR. Since CD8-B7-2-A2 has two lysine residues, K340 and K364, at its cytoplasmic tail, which are candidates for the ubiquitination site, these candidate sites were mutated to arginine simultaneously or one by one. Each CD8-B7-

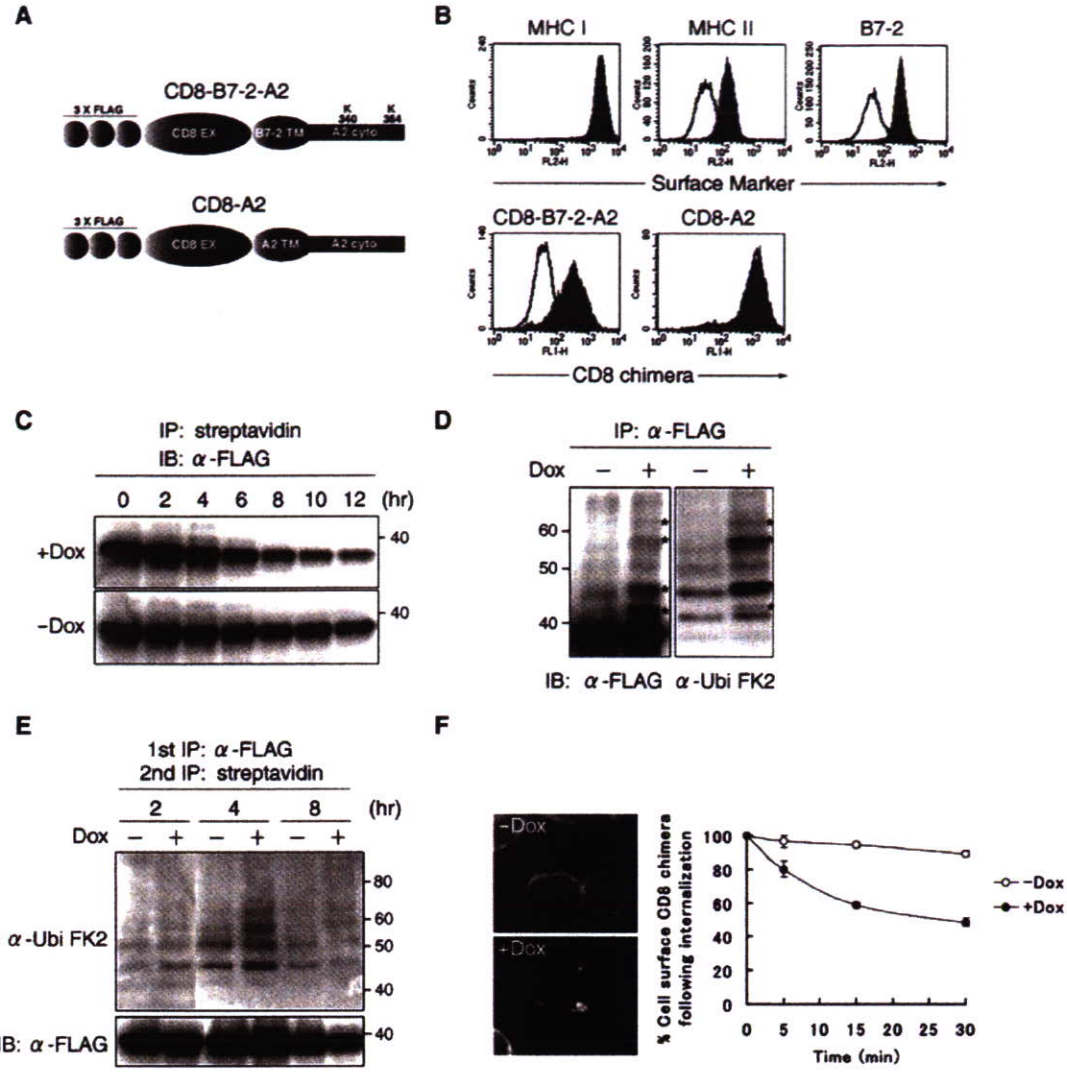


**Figure 1. Generation of T-REx-c-MIR.** **(A)** Schematic representation of the structure of CD8 chimeras used in this experiment. Extracellular domain (EX), transmembrane domain (TM), and cytoplasmic tail (cyto) are indicated. **(B)** After being incubated with and without Dox for 24 hr, the expression level of indicated surface molecules on T-REx-c-MIR was examined by FACS. Data from the cells incubated with Dox (open histograms), and the cells incubated without Dox (shaded histograms) are shown. Data are representative of two independent experiments. **(C)** Surface molecules of T-REx-c-MIR were biotinylated first. After biotinylated T-REx-c-MIR was incubated with or without Dox for the indicated periods of times, biotinylated proteins were purified with streptavidin-agarose and analyzed with anti-FLAG Ab. Upper and lower panels showed the results from the cells incubated with and without Dox, respectively. Data are representative of two independent experiments. **(D)** Whole cell lysate extracted from T-REx-c-MIR that was cultivated with or without Dox for 6 hr was incubated with anti-FLAG Ab. Precipitated samples were probed with anti-FLAG Ab (left) or anti-ubiquitin Ab (right). Bands corresponding to the ubiquitinated CD8-B7-2-A2 is are marked by an asterisk (*) as shown. **(E)** Surface molecules of T-REx-c-MIR were biotinylated as in C. After biotinylated T-REx-c-MIR was incubated with (+) or without (−) Dox for the indicated periods of time, biotinylated proteins were sequentially purified with anti-FLAG Ab and streptavidin-agarose. Each sample was probed with anti-ubiquitin Ab (upper) and anti-FLAG Ab (lower). Data are representative of two independent experiments. **(F)** T-REx-c-MIR was incubated with Dox for 6 hr and cultivated in the presence of FITC-conjugated anti-CD8 Ab for the last 10 min. Internalized CD8-B7-2-A2 was observed with a fluorescence microscope (left panel). For the quantitative analysis of internalization, surface CD8-B7-2-A2 of T-REx-c-MIR was labeled with anti-CD8 Ab after being incubated with (+) or without (−) Dox for 6 hr. After cultivation at 37°C for the indicated times, the expression of remaining surface CD8-B7-2-A2 was examined by staining with PE-conjugated goat anti-mouse IgG. At each point, the percentage of remaining CD8-B7-2-A2 was calculated relative to the value of labeled CD8-B7-2-A2 at 0 min (right panel).
doi:10.1371/journal.pone.0001490.g001

2-A2 mutant was stably expressed in T-REx-c-MIR and assayed. Eight hours after induction by Dox, the surface expression of each CD8-B7-2-A2 mutant was examined by FACS analysis. As shown in Figure 3A, the CD8-B7-2-A2 mutant whose two lysine residues were simultaneously mutated to arginine, named CD8-B7-2-$A2^{K340R, K364R}$, was not down-regulated at all. Among the two responsible lysine residues, K340 had a greater effect than K364 in down-regulating the target molecule (Figure 3A).

To investigate whether the inhibition of down-regulation is due to less ubiquitination, the status of ubiquitination of CD8-B7-2-A2 mutants was examined, as performed in Figure 1D. As shown in Figure 3B, the status of ubiquitination of CD8-B7-2-$A2^{K340R, K364R}$, which was purified from whole cell lysate, was not changed by Dox-induced c-MIR expression. Furthermore, the status of ubiquitination of CD8-B7-2-$A2^{K340R, K364R}$ was different from that of CD8-B7-2-A2 even without adding Dox; the two

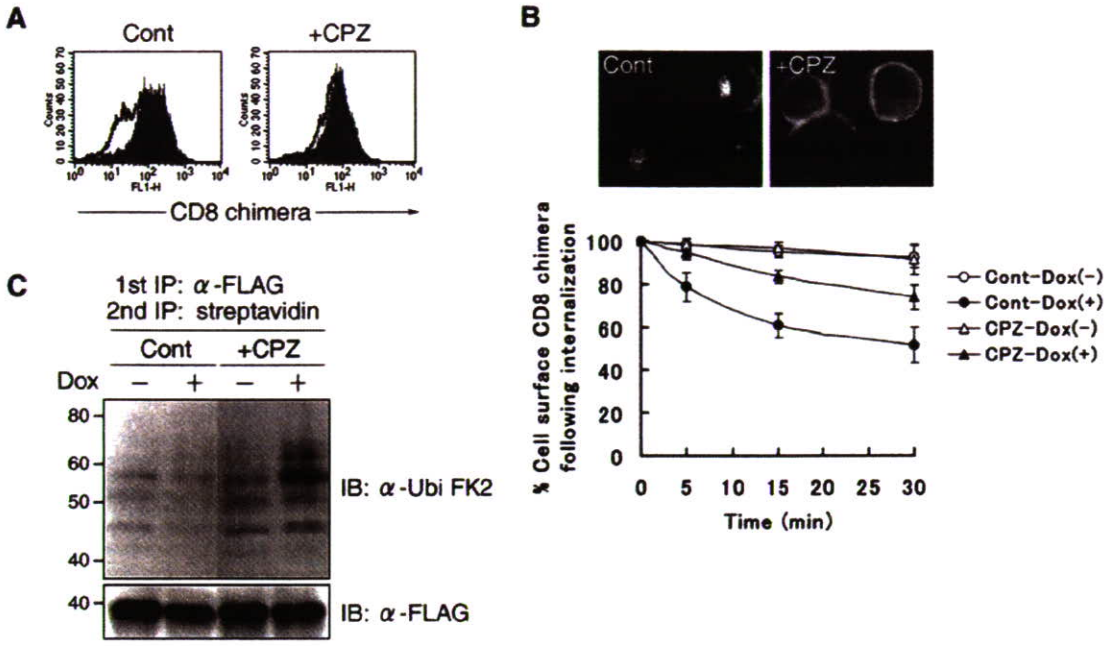


**Figure 2. Accumulation of ubiquitinated surface CD8 chimera by inhibiting internalization.** **(A)** After being incubated with or without Dox for 3 hr, T-REx-c-MIR was further cultivated for 5 hr with chlorpromazine (10 μg/ml) (+CPZ) or water (Cont) in the presence or absence of Dox. At the end of incubation, the expression of surface CD8-B7-2-A2 on T-REx-c-MIR was examined by FACS. Data from cells incubated with Dox (open histograms) and cells incubated without Dox (shaded histograms) are shown. Data are representative of two independent experiments. **(B)** T-REx-c-MIR was treated as in A. Treated T-REx-c-MIR was incubated in the presence of FITC-conjugated CD8 Ab at 37°C for 10 min, and internalized CD8-B7-2-A2 was examined by fluorescence microscopy. For the quantitative analysis of internalization, surface CD8-B7-2-A2 of T-REx-c-MIR treated as above was labeled with anti-CD8 Ab, and cultivated at 37°C for the indicated times. The expression of remaining surface CD8-B7-2-A2 was examined by staining with PE-conjugated goat anti-mouse IgG. At each point, the percentage of remaining CD8-B7-2-A2 was calculated as in Figure 1F. **(C)** Surface molecules of T-REx-c-MIR were biotinylated first as in Figure 1C. After biotinylated T-REx-c-MIR was incubated with (+) or without (−) Dox for 3 hr, biotinylated T-REx-c-MIR was further cultivated with chlorpromazine (10 μg/ml) (+CPZ) or water (Cont) for 5 hr in the presence (+) or absence (−) of Dox. After cultivation, biotinylated CD8-B7-2-A2 was sequentially purified with anti-FLAG Ab and streptavidin-agarose. Each sample was probed with anti-ubiquitin Ab (upper panel) or anti-FLAG Ab (lower panel). Data are representative of two independent experiments.
doi:10.1371/journal.pone.0001490.g002

bands marked with small triangles in the right panel of Figure 3B and C disappeared in CD8-B7-2-A2$^{K340R, K364R}$. Those bands also disappeared in CD8-B7-2-A2$^{K364R}$, in which K364 of CD8-B7-2-A2 was mutated to arginine, demonstrating that the ubiquitination of K364 takes place in the steady state (Figure 3C). On the other hand, the bands that appeared due to Dox-induced c-MIR (marked with * in Figure 3B and C) disappeared in CD8-B7-2-A2$^{K340R}$, in which K340 of CD8-B7-2-A2 was mutated to arginine (Figure 3C). This was also the case in the surface CD8-B7-2-A2 mutants (Figure 3D). Together, the results indicate that Dox-induced c-MIR promotes internalization of CD8-B7-2-A2 most likely through ubiquitination at K340.

To confirm this, we examined the internalization rate of each mutant. As shown in Figure 3E, the internalization rate of CD8-B7-2-A2$^{K340R, K364R}$ was the lowest among the mutants examined. Consistent with the results shown in Figure 3A, the internalization rate of CD8-B7-2-A2$^{K340R}$ was lower than that of CD8-B7-2-A2$^{K364R}$. Taken together, these results strongly suggest that ubiquitination at K340 mainly contributes to c-MIR-mediated internalization.

## Inhibition of surface ubiquitination weakens internalization

The results obtained by analysis with mutant target molecules support the idea that surface ubiquitination functions as an internalization signal in T-REx-c-MIR, but must be interpreted with care. Lysine residues might be modulated by a conjugation system that has not yet been identified to this day. Therefore, we examined the effect of inhibiting surface ubiquitination on the internalization rate of CD8-B7-2-A2. It was demonstrated that UbcH5b and c are responsible ubiquitin conjugating enzymes for MIR1, a viral ubiquitin ligase that belongs to the same family as c-MIR [15]. Also, we showed that the RINGv domain of c-MIR can function as an E3 catalytic domain of MIR1 [11]. Therefore, we examined the possibility that c-MIR also utilizes UbcH5b and c as ubiquitin conjugating enzymes, using the retroviral transduction method.

T-REx-c-MIR, whose UbcH5b/c expression was knocked down, was generated by infection with a retrovirus that expresses shRNA against both UbcH5b and c (Figure 4A). c-MIR was expressed by adding Dox in knocked down T-REx-c-MIR, and the surface expression of CD8-B7-2-A2 was examined. As we expected, the down-regulation of CD8-B7-2-A2 was significantly inhibited in knocked down T-REx-c-MIR compared with T-REx-c-MIR infected with control shRNA-expressing retrovirus (Figure 4A). In both cells, the expression of c-MIR was equivalent (Figure 4A). Therefore, we employed shRNA for UbcH5b/c to inhibit c-MIR-mediated ubiquitination. As shown in Figure 4C, D, surface CD8-B7-2-A2 was less ubiquitinated and was less internalized in knocked down T-REx-c-MIR compared with control cells. These results clearly demonstrate that surface ubiquitination is necessary for internalization of surface CD8 chimera.

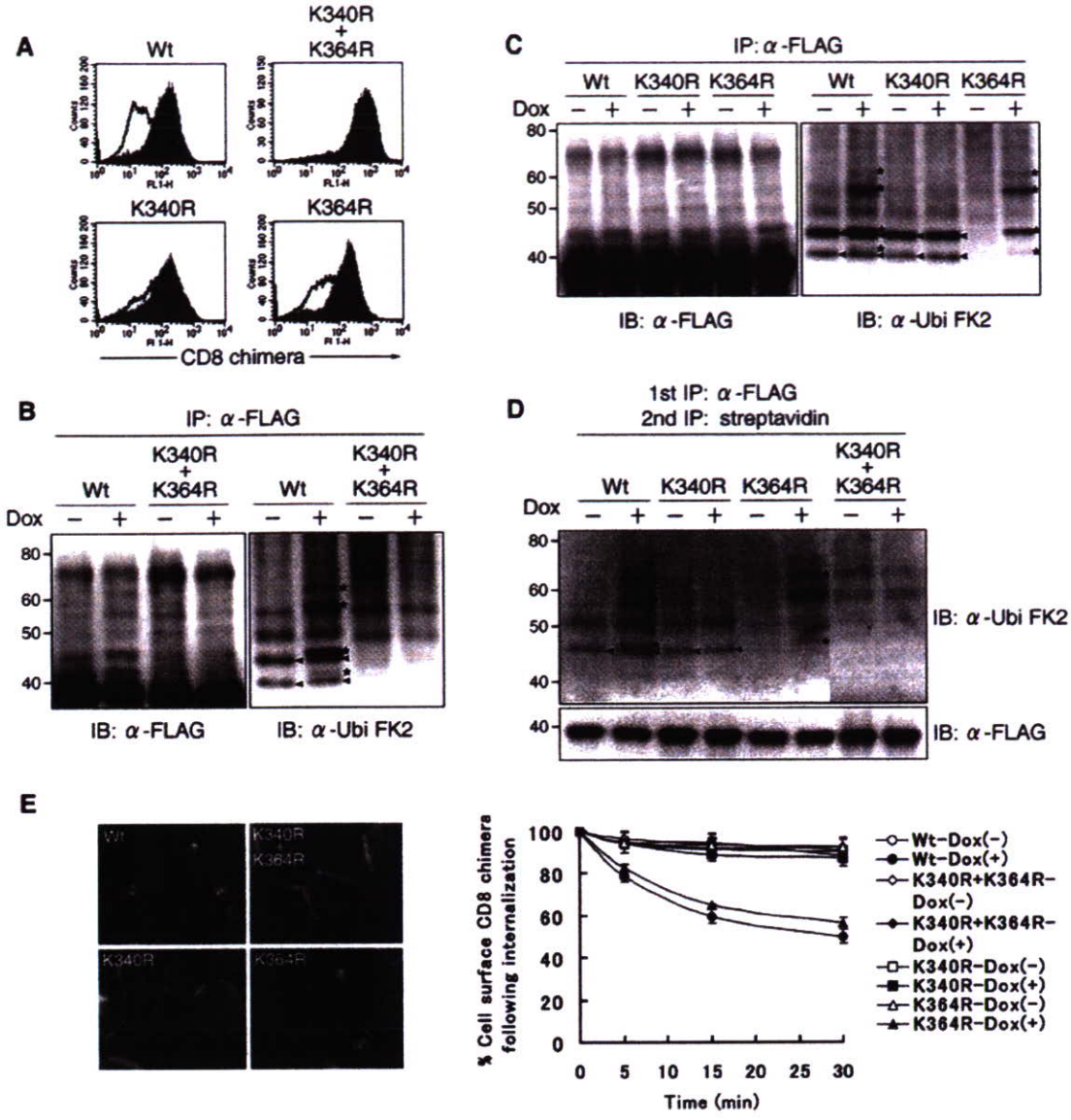


**Figure 3. Lysine-less target molecules are neither ubiquitinated nor internalized in T-REx-c-MIR. (A)** After being incubated with and without Dox for 8 hr, the expression of indicated surface molecules on T-REx-c-MIR was examined by FACS. Data from cells incubated with Dox (open histograms) and cells incubated without Dox (shaded histograms) are shown. Data are representative of two independent experiments. **(B) (C)** Whole cell lysate extracted from indicated CD8-chimera-expressing T-REx-c-MIR that was cultivated with or without Dox for 6 hr was incubated with anti-FLAG Ab. Precipitated samples were probed with anti-FLAG Ab (left) or anti-ubiquitin Ab (right). Bands corresponding to newly and constitutively ubiquitinated CD8-B7-2-A2 are marked with an asterisk (*) and small triangles, respectively (shown in right panels). **(D)** Surface molecules of indicated CD8-chimera-expressing T-REx-c-MIR were biotinylated first as in Figure 1C. After each biotinylated T-REx-c-MIR was incubated with (+) or without (−) Dox for 4 hr, biotinylated proteins were sequentially purified with anti-FLAG Ab and streptavidin-agarose. Each sample was probed with anti-ubiquitin Ab or anti-FLAG Ab. Data are representative of two independent experiments. Bands corresponding to newly and constitutively ubiquitinated surface CD8-B7-2-A2 are marked with an asterisk (*) and small triangles, respectively. **(E)** Indicated CD8-chimera-expressing T-REx-c-MIR was incubated with Dox for 6 hr and cultivated in the presence of FITC-conjugated anti-CD8 Ab for the last 10 min. Internalized CD8 chimera was observed by fluorescence microscopy (left panel). For the quantitative analysis of internalization, each T-REx-c-MIR was incubated with (+) or without (−) Dox for 6 hr, and surface CD8 chimera of T-REx-c-MIR was labeled with anti-CD8 Ab. After each labeled T-REx-c-MIR was cultivated at 37°C for the indicated times, the percentage of remaining CD8-B7-2-A2 was calculated as in Figure 1F (right panel).
doi:10.1371/journal.pone.0001490.g003

## Complex formation between CD8 chimera target and c-MIR at plasma membrane

Lastly, we examined whether CD8-B7-2-A2 forms a complex with c-MIR at the plasma membrane. As negative control, CD8-A2 was employed because it does not bind to c-MIR and therefore is not ubiquitinated by c-MIR [11]. Surface molecules of T-REx-c-MIR, which constitutively express CD8-B7-2-A2 or CD8-A2, were biotinylated after c-MIR was expressed by adding Dox, and the protein complex including biotinylated CD8-B7-2-A2 or CD8-A2 was purified with streptavidin beads and anti-FLAG M2 beads. Purified protein complex was subjected to western blot analysis with anti-V5 and anti-FLAG Abs to detect c-MIR and CD8 chimeras, respectively. As shown in Figure 5A, c-MIR was

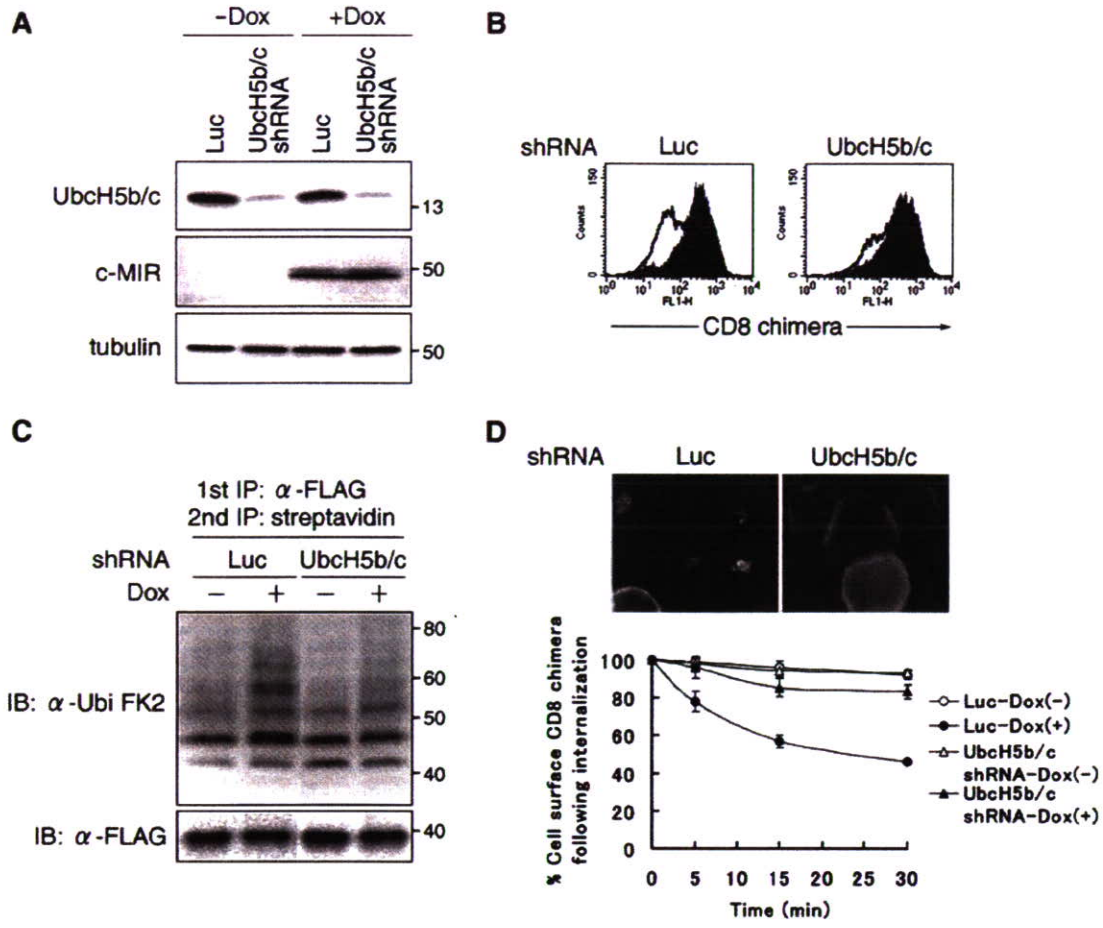


**Figure 4. Inhibition of surface ubiquitination weakens internalization.** **(A)** Control shRNA (Luc) or shRNA for UbcH5b and c (UbcH5b/c) was retrovirally transduced into T-REx-c-MIR. Whole cell lysate from each indicated T-REx-c-MIR was analyzed with anti-UbcH5, V5 (for c-MIR), and tubulin Abs 6 hr after incubation with or without Dox. Data are representative of two independent experiments. **(B)** Indicated T-REx-c-MIR was incubated with or without Dox for 8 hr and the expression of CD8-B7-2-A2 was analyzed by FACS. Data are representative of two independent experiments. **(C)** Surface molecules of T-REx-c-MIR treated with indicated shRNA were biotinylated first as in Figure 1C. After biotinylated T-REx-c-MIR was incubated with (+) or without (−) Dox for 4 hr, biotinylated CD8-B7-2-A2 was sequentially purified with anti-FLAG Ab and streptavidin-agarose. Each sample was probed with anti-ubiquitin Ab or anti-FLAG Ab. Data are representative of two independent experiments. **(D)** Indicated T-REx-c-MIR was incubated with Dox for 6 hr and cultivated in the presence of FITC-conjugated anti-CD8 Ab for the last 10 min. Internalized CD8 chimera was observed by fluorescence microscopy (upper panel). For the quantitative analysis of internalization, indicated T-REx-c-MIR was incubated with (+) or without (−) Dox for 6 hr, and surface CD8-B7-2-A2 of T-REx-c-MIR was labeled with anti-CD8 Ab. After cultivation at 37°C for the indicated times, the percentage of remaining CD8-B7-2-A2 was calculated as in Figure 1F (lower panel).
doi:10.1371/journal.pone.0001490.g004

detected in the protein complex containing surface CD8-B7-2-A2, but not in the protein complex containing surface CD8-A2. Furthermore, we examined whether c-MIR is present at the plasma membrane. After c-MIR was expressed by adding Dox, surface molecules of T-REx-c-MIR were biotinylated. Expressed c-MIR was purified with anti-V5 Ab and analyzed with HRP-conjugated streptavidin. As shown in Figure 5B, biotinylated c-MIR was clearly detected. These results demonstrate that c-MIR associates with CD8-B7-2-A2 at the plasma membrane.

## DISCUSSION

Here, we reported a useful experimental tool named as T-REx-c-MIR for monitoring the internalization induced by surface ubiquitination. This construction was achieved by employing a constitutively active E3 ubiquitin ligase, c-MIR. Given that impaired ubiquitin-mediated regulation of growth factor receptors is suggested to cause several diseases including malignancies [6], the molecular machinery of ubiquitin-mediated internalization, which will be revealed by using T-REx-c-MIR, will provide new insights into strategies for treatment of human diseases.

In mammals, it is difficult to reveal molecular basis for ubiquitination-mediated internalization, because it has been difficult to obtain the proof that surface ubiquitination functions an internalization signal for the following reasons. One is the presence of possible redundant pathways for the internalization of surface molecules in mammals. For instance, in the case of the EGF receptor (EGFR) that is under intensive investigation, two machineries for internalization have been proposed [3]. The first one is the c-Cbl-mediated ubiquitination of EGFR, where the binding of EGF to EGFR induces auto-phosphorylation of several cytoplasmic tyrosine residues of EGFR and recruits c-Cbl, a ubiquitin ligase, through the SH-2 domain of c-Cbl, thereby ubiquitinating EGFR at multiple cytoplasmic lysine residues and inducing internalization. The second one is the CIN-85-mediated internalization, where, upon receptor activation, EGFR-associated c-Cbl recruits endophilin through an adaptor molecule, CIN-85,

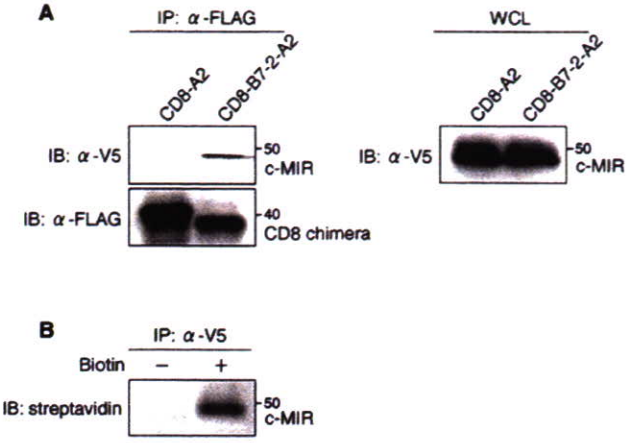


**Figure 5. c-MIR binds to CD8 chimera target at plasma membrane. (A)** Indicated CD8-chimera-expressing T-REx-c-MIR was incubated with Dox for 4 hr, and surface molecules of T-REx-c-MIR were biotinylated as in Figure 1C. Protein complex including biotinylated CD8 chimera was sequentially purified with anti-FLAG Ab and streptavidin-agarose. Each sample was probed with anti-V5 Ab and anti-FLAG Ab (left panel). Whole cell lysate from each T-REx-c-MIR was analyzed with anti-V5 Ab (right panel). Data are representative of two independent experiments. **(B)** T-REx-c-MIR was incubated with Dox for 4 hr, and surface molecules of T-REx-c-MIR were biotinylated. c-MIR proteins were purified with anti-V5 Ab and analyzed with HRP-conjugated streptavidin. Data are representative of two independent experiments.
doi:10.1371/journal.pone.0001490.g005

thereby facilitating the invagination of plasma membrane [16]. This possible redundant pathway might explain why the inhibition of EGFR ubiquitination by v-Cbl, a dominant-negative form of c-Cbl, is not able to inhibit the internalization of EGFR [17,18]. Another reason is the absence of a suitable experimental tool by which the detailed status of ubiquitination of surface molecules can be visualized. Although there are a few reports in which the ubiquitination status of surface molecules is monitored by using surface biotinylation, they only demonstrated that ubiquitinated target molecules are present at the plasma membrane [19,20]. Given that it is necessary to show that non-ubiquitinated target surface molecules undergo ubiquitination immediately before the initiation of internalization, the evidence presented in those studies is not strong enough. Indeed, ubiquitin-harboring model membrane proteins, which are generally employed to analyze ubiquitin-mediated traffic, are able to reach the plasma membrane [21], indicating that some molecules ubiquitinated inside the cells might be transported to the plasma membrane.

In order to overcome the problems mentioned above, we utilized c-MIR, a constitutively active E3 ubiquitin ligase, for B7-2 and MHC II [11–13]. We previously showed that transient or stable over-expression of c-MIR induces marked internalization of target surface molecules, and its effect is cancelled by inhibition of target molecule ubiquitination. Based on these findings, we had proposed that c-MIR is a constitutively active E3 ubiquitin ligase and induces the internalization of a surface molecule through ubiquitination of its cytoplasmic tail [11]. c-MIR belongs to a novel family of membrane-bound ubiquitin ligases designated as the MIR/K3 family [14,22]. All MIR family members possess a variant type of RING (RINGv) domain as an E3 catalytic domain and two transmembrane regions at the amino terminus and the center, respectively. Each MIR family member has specific target molecules: B7-2 and MHC II for c-MIR, and MHC I for MIR1 and 2 [11,13,23–25]. Previous reports have shown that MIR family members ubiquitinate target molecules through association between the transmembrane regions of E3 and their targets, but it remains unknown how the association is regulated [11,26]. Our present data showed that T-REx-c-MIR also can be utilized to reveal how c-MIR recognizes the substrate.

To monitor the surface ubiquitination-induced internalization, we employed the exogenously expressed CD8 chimeric molecules as we could not monitor the ubiquitination status of endogenous target molecules (e.g. B7-2) unless the inhibitor for degradation was used in T-REx-c-MIR (Figure S1). Therefore, there is the possibility that the exogenously expressed CD8 chimeric molecules might induce artificial effects (e.g. ER stress) to T-REx-c-MIR, thereby the results obtained from CD8 chimeric molecules-expressing T-REx-c-MIR might not reflect the authentic events observed in the endogenous target molecules (e.g. B7-2, MHC class II). To exclude this possibility, we compared CD8 chimera-expressing T-REx-c-MIR with original T-REx-c-MIR. Both T-REx-c-MIRs showed same phenotypes in terms of down-regulation, ubiquitination status and endocytosis of B7-2 (Figure S2A, B and C). Also, the extent of ER stress was not increased by expression of CD8 chimera (Figure S2D). These results demonstrated that the result obtained in this experiment is not totally artificial one.

Although we previously reported c-MIR as an E3 ubiquitin ligase, c-MIR might have other functions than E3 ubiquitin ligase. Indeed, c-Cbl facilitates internalization of EGFR through binding to CIN-85, and its function does not depend on the E3 ubiquitin ligase activity of c-Cbl [16]. Therefore, we examined the relationship between ubiquitination activity and internalization activity by using several c-MIR mutants. We generated c-MIR mutant whose RINGv domain was mutated (Figure S3A). Also, additional c-MIR mutant whose first hypothetical tyrosine-based motif (Y1) or second hypothetical tyrosine-based motif (Y2) was deleted was generated (Figure S3A). As shown in Figure S3B, C, all c-MIR mutants could not down-regulate and ubiquitinate the target molecules. These results support our idea that c-MIR-mediated internalization depends on the ubiquitin ligase activity of c-MIR in T-REx-c-MIR.

T-REx-c-MIR and FLAG-tagged target molecules present several advantages for the investigation of ubiquitin-mediated membrane trafficking [13,27]. By combining with the surface biotinylation method, we succeeded for the first time in observing in detail the status of target ubiquitination. Also, the purification method with M2-conjugated matrix is a convenient and excellent means to detect ubiquitinated target molecules. As shown in Figure 3, this method allowed us to conclude that K340 is the dominant site of ubiquitination by c-MIR. In addition, T-REx-c-MIR can be easily modified by retrovirus-mediated gene transfer. We observed that around 80% of the cells were infected with reporter-expressing retrovirus, as judged by the expression of a reporter gene (data not shown). Thus, T-REx-c-MIR can be employed to test whether candidate molecules are indeed involved in ubiquitin-mediated transport.

In this study, we found that c-MIR-mediated internalization was inhibited by chlorpromazine and dansylcadaverine, which are inhibitors of clathrin-dependent internalization. In contrast, nystatin and filipin, which are inhibitors of caveolin-dependent internalization, did not inhibit c-MIR-mediated internalization (data not shown). Also, oligo-ubiquitinated target surface molecules were accumulated by inhibiting internalization (Figure 2C). These results support previous reports demonstrating that the oligo-ubiquitination of plasma membrane proteins induces clathrin-dependent internalization [15,21].

Our present results give rise to several important points in ubiquitination-mediated internalization. As shown in Figure 3C, the ubiquitination of K364 constitutively took place, but was not a

strong internalization signal. In contrast, the ubiquitination of K340 was induced by Dox-mediated c-MIR expression, and was an essential signal for internalization. These results indicated that the ubiquitination of K364 is induced by unidentified endogenous E3 ubiquitin ligases in T-REx-c-MIR. Interestingly, K340 was also demonstrated to be a critical residue for internalization induced by MIR1, viral MIR family member [28]. At present, we cannot explain the difference in the ability to induce internalization between K340 and K364. Nevertheless, we would like to propose that effective internalization requires lysine residues suitably positioned at cytoplasmic tail of the target molecule and a suitable form of ubiquitination chain at critical lysine residues.

## MATERIALS AND METHODS

### Plasmid construction

Each CD8 chimera was constructed by overlapping PCR as described previously [11]. Substitutions were engineered into CD8 chimera by PCR-based mutagenesis (Promega). Each cDNA of CD8 chimera was subcloned into p3XFLAG-CMV vector (Sigma) to introduce a FLAG epitope tag at the amino terminus. shRNA for UbcH5b/c or luciferase was first subcloned into pcPUR vector [29], and each shRNA cassette was transferred into pSIREN-puro vector (BD). To generate shRNA for UbcH 5b/c, we employed the sequence reported to be able to inhibit both UbcH5b and UbcH5c [15].

### Generation of T-REx-c-MIR

To generate T-REx-c-MIR, BJAB cells were utilized as parent cells. Generation of T-REx-c-MIR cells was performed using the Flp-In ™ T-REx ™ Core Kit (Invitrogen). All procedures were in accordance with the manufacturer's recommendation. His-V5-tagged human c-MIR-expressing cassette, which was used in our previous report [11], was transferred into pcDNA5/FRT/TO vector. Each c-MIR mutant was constructed by overlapping PCR and transferred into pcDNA5/FRT/TO vector [11]. Generated T-REx-c-MIR was transfected with CD8-chimera-expressing plasmids constructed in p3xFLAG-CMV vector, and CD8-chimera-expressing T-REx-c-MIR was selected by incubation with 2 mg/ml G418 (Sigma) for 3–6 weeks.

### Induction of c-MIR in T-REx-c-MIR

T-REx-c-MIR ($3\times10^5$/ml) was incubated with 1 μg/ml doxycycline (Sigma) in 10% FCS-containing RPMI (Sigma) for indicated times.

### Flow cytometry analysis and antibody

Cells ($5\times10^5$) were washed with PBS containing 2% fetal calf serum (FCS) and incubated with FITC- or phycoerythrin (PE)-conjugated monoclonal Abs for 30 min at 4°C. After being washed, each sample was fixed with 2% paraformaldehyde solution and flow cytometry analysis was performed with FACSCalibur (BD Biosciences). W6/32 Ab for MHC I, RPA-T8 Ab for CD8, FUN-1 Ab for B7-2, and TÜ36 Ab for MHC II used for FACScan were obtained from BD Biosciences. M2 anti-FLAG Ab (Sigma), F7 anti-HA Ab (Santa Cruz), G-18 anti-His Ab (Santa Cruz), FK2 anti-ubiquitin Ab (AFFINITI Research Products) and anti-V5 Ab (Invitrogen) were used for immunoprecipitation and/or immunoblot analysis.

### Cell surface biotinylation

Cells were incubated with Sulfo-NHS-biotin (2 mg/ml) (Pierce) in PBS (pH 8.0) for 30 min on ice. After incubation, excess biotin was quenched with ice-cold 100 mM glycin. After being chased for the indicated times at 37°C, surface biotinylated cells were used in each experiment.

### Detection of ubiquitinated CD8 chimera

In order to detect the ubiquitination of CD8 chimera, cell pellet was boiled in 1% SDS-containing RIPA buffer (10 mM Tris (pH 7.5), 1% NP40, 0.1% DOC, 0.15 M NaCl, 1 mM EDTA (pH 8.0)), and diluted 10-fold with SDS-free RIPA buffer. After removing cell debris, CD8 chimeric molecules were precipitated with M2 anti-FLAG Ab-coupled sepharose (Sigma). The precipitated CD8 chimeric molecules were eluted with FLAG peptide (150 μg/ml). The eluted sample was subjected to western blot analysis with M2 anti-FLAG Ab or FK2 anti-ubiquitin Ab. To examine whether CD8 chimeric molecules that pre-exists at the plasma membrane before initiation of ubiquitination process by c-MIR are ubiquitinated, surface molecules of CD8-chimera-expressing T-REx-c-MIR cells were biotinylated and followed by incubation with Dox. After being incubated for indicated time, CD8 chimera was purified with M2 anti-FLAG Ab- coupled sepharose as performed above, and further purified with streptavidin-agarose (Pierce), and subjected to western blot analysis with M2 anti-FLAG Ab or FK2 anti-ubiquitin Ab.

### Analysis of surface CD8 chimera stability

Cells were biotinylated as above and cultured in 10% FCS RPMI at 37°C for indicated times. At the end of the chase periods, biotinylated proteins were extracted with 0.1% SDS containing RIPA buffer, purified with streptavidin-agarose, and subjected to western blot with M2 anti-FLAG Ab.

### Internalization assay

Cells were stained with anti-CD8 Ab for 30 min at 4°C. After being washed, cells were cultured for indicated times at 37°C and stained with PE-conjugated goat anti-mouse IgG Ab, followed by FACS analysis at each time point. The absolute value of the surface expression level was determined by subtracting the mean fluorescence intensity (MFI) of cells stained with isotype control Ab from the MFI of cells stained with anti-CD8 Ab. The percentage of CD8 chimera remaining at the cell surface was obtained by dividing the values obtained at each incubation period by the value obtained at time zero. For immunofluorescence microscopy, FITC-labeled CD8 Ab was added to the culture medium of T-REx-c-MIR, and T-REx-c-MIR was cultivated for 10 min at 37 . After being washed, these cells were subjected to analysis with an immunofluorescence microscope.

### Knock-down of E2 by shRNA

Inhibition of E2 ubiquitin conjugating enzymes was performed by retroviral transduction of shRNAs against UbcH5b/c. shRNA-expressing retrovirus was generated by transfecting pSIREN vector that expresses shRNA against UbcH5b/c or control molecule, luciferase, into Phoenix packaging cells. T-REx-c-MIR was infected by spin infection (2,000 rpm for 1 hr at 32°C) with each shRNA-expressing retrovirus. shRNA-expressing T-REx-c-MIR cells were selected by adding puromycin (4 μg/ml).

## SUPPORTING INFORMATION

**Figure S1** Detection of ubiquitinated B7-2 in T-REx-c-MIR. Original T-REx-c-MIR were incubated with Dox for 8 hr, and cell pellet of incubated original T-REx-c-MIR was boiled in 1% SDS-containing RIPA buffer (10 mM Tris (pH 7.5), 1% NP40, 0.1% DOC, 0.15 M NaCl, 1 mM EDTA (pH 8.0)), and diluted 10-fold with SDS-free RIPA buffer. After removing cell debris,

endogenous B7-2 molecule was precipitated with IT 2.2 anti-B7-2 Ab. The precipitated sample was subjected to western blot analysis with BU63 anti-B7-2 Ab or FK2 anti-ubiquitin Ab. Same experiments were performed after degradation of B7-2 was inhibited by adding 2 μM of bafilomycin A1 (Bafi-A1+). In that case, original T-REx-c-MIR was incubated with Dox for 8 hr, and incubated with bafilomycin A1 for the last 5 hr.
Found at: doi:10.1371/journal.pone.0001490.s001 (0.20 MB TIF)

**Figure S2** Comparison between original T-REx-c-MIR and CD8 chimera-expressing T-REx-c-MIR. (A) Indicated T-REx-c-MIRs were incubated with Dox for 24 hr, and the expression level of surface B7-2, MHC class I (MHC I) and MHC class II (MHC II) was analyzed by FACS. Data from the cells incubated with Dox (open histograms), and the cells incubated without Dox (shaded histograms) are shown. "T-REx-c-MIR" indicates original T-REx-c-MIR. "T-REx-c-MIR-CD8-B7-2-A2" indicates CD8 chimera-expressing T-REx-c-MIR. (B) Original T-REx-c-MIR and CD8 chimera-expressing T-REx-c-MIR were incubated with Dox for 8 hr, and incubated with 2 μM of bafilomycin A1 for the last 5 hr. After incubation, whole cell lysate extracted from each T-REx-c-MIR was incubated with IT 2.2 anti-B7-2 Ab. Precipitated samples were probed with FK-2 anti-ubiquitin Ab (upper) or BU63 anti-B7-2 Ab (lower). The results of original T-REx-c-MIR and CD8 chimera-expressing T-REx-c-MIR were shown in lane 1 and 2 and lane 3 and 4, respectively. (C) Indicated T-REx-c-MIRs were incubated with Dox for 8 hr and cultivated in the presence of FITC-conjugated FUN-1 anti-B7-2 Ab for the last 10 min. Internalized B7-2 was observed with a fluorescence microscope (lower panel). For the quantitative analysis of internalization, surface B7-2 of each T-REx-c-MIR was labeled with FUN-1 anti-B7-2 Ab after being incubated with (+) or without (−) Dox for 8 hr. After cultivation at 37°C for the indicated times, the expression of remaining surface B7-2 was examined by staining with PE-conjugated goat anti-mouse IgG. At each point, the percentage of remaining B7-2 was calculated relative to the value of labeled CD8-B7-2-A2 at 0 min (upper panel). (D) Total RNA from T-REx-c-MIR or CD8 chimera-expressing T-REx-c-MIR either unstimulated (−) or stimulated (+) with Tunicamycin (Tm) (2.5μg/ml) as positive control for 24 h (upper panel) or 12 h (lower panel) was used for RT-PCR analysis. In the upper panel, RT-PCR analysis of XBP1 mRNA splicing was done with a primer set flanking the spliced-out region in XBP1 mRNA. PCR products separated by electrophoresis on 3% agarose gel. In the lower panel, the abundance of GRP78 mRNA was determined by semi-quantitative RT-PCR analysis. PCR products were resolved on 1.5% agarose gel. The results of original T-REx-c-MIR and CD8 chimera-expressing T-REx-c-MIR were shown in lane 1, 3, 5, 7, 9, 11and lane 2, 4, 6, 8, 10, 12, respectively. XBP1(h), hybrid of spliced and unspliced; XBP1(u), unspliced; XBP1(s), spliced; ACTB; beta-actin.
Found at: doi:10.1371/journal.pone.0001490.s002 (1.66 MB TIF)

**Figure S3** Analysis of c-MIR mutants. (A) Schematic representation of the structure of c-MIR mutants used in this experiment. First putative tyrosine based motif (Y1), second putative tyrosine based motif (Y2), transmembrane domain (TM), and variant RING domain (RINGv) are indicated. (B) Each T-REx-c-MIR expressing indicated c-MIR mutant was incubated with Dox for 24 hr, and the expression level of surface CD8-B7-2-A2 was examined by FACS. (C) Each T-REx-c-MIR was incubated with Dox for 6 hr, and CD8-B7-2-A2 molecules were purified from whole cell lysate as performed in Figure 1D. Purified CD8-B7-2-A2 was analyzed with M2 anti-FLAG and FK2 anti-ubiquitin Abs (upper panel). Bands corresponding to the ubiquitinated CD8-B7-2-A2 is are marked by an asterisk (*) as shown. Also, the expression level of each c-MIR mutant was analyzed by western blot analysis with anti-V5 Ab (lower panel).
Found at: doi:10.1371/journal.pone.0001490.s003 (1.60 MB TIF)

## ACKNOWLEDGMENTS

We thank S. Yamasaki for providing Phoenix packaging cells and technical advice, and K. Nakamura and S. Dohi for manuscript preparation.

## Author Contributions

Conceived and designed the experiments: SI EG. Performed the experiments: EG MM MA MU. Analyzed the data: MM. Contributed reagents/materials/analysis tools: YM MO HH MM. Wrote the paper: SI EG.

## REFERENCES

1. Hershko A, Ciechanover A (1998) The ubiquitin system. Annu Rev Biochem 67: 425–479.
2. Chau V, Tobias JW, Bachmair A, Marriott D, Ecker DJ, et al. (1989) A multiubiquitin chain is confined to specific lysine in a targeted short-lived protein. Science 243: 1576–1583.
3. Dupre S, Urban-Grimal D, Haguenauer-Tsapis R (2004) Ubiquitin and endocytic internalization in yeast and animal cells. Biochim Biophys Acta 1695: 89–111.
4. Mukhopadhyay D, Riezman H (2007) Proteasome-independent functions of ubiquitin in endocytosis and signaling. Science 315: 201–205.
5. Thien CB, Langdon WY (2005) c-Cbl and Cbl-b ubiquitin ligases: substrate diversity and the negative regulation of signaling responses. Biochem J 391: 153–166.
6. Ryan PE, Davies GC, Nau MM, Lipkowitz S (2006) Regulating the regulator: negative regulation of Cbl ubiquitin ligases. Trends Biochem Sci 31: 79–88.
7. Ridge SA, Worwood M, Oscier D, Jacobs A, Padua RA (1990) FMS mutations in myelodysplastic, leukemic, and normal subjects. Proc Natl Acad Sci U S A 87: 1377–1380.
8. Baker A, Cachia P, Ridge S, McGlynn H, Clarke R, et al. (1995) FMS mutations in patients following cytotoxic therapy for lymphoma. Leuk Res 19: 309–318.
9. Hicke L, Dunn R (2003) Regulation of membrane protein transport by ubiquitin and ubiquitin-binding proteins. Annu Rev Cell Dev Biol 19: 141–172.
10. Hicke L, Riezman H (1996) Ubiquitination of a yeast plasma membrane receptor signals its ligand-stimulated endocytosis. Cell 84: 277–287.
11. Goto E, Ishido S, Sato Y, Ohgimoto S, Ohgimoto K, et al. (2003) c-MIR, a human E3 ubiquitin ligase, is a functional homolog of herpesvirus proteins MIR1 and MIR2 and has similar activity. J Biol Chem 278: 14657–14668.
12. Bartee E, Mansouri M, Hovey Nerenberg BT, Gouveia K, Fruh K (2004) Downregulation of major histocompatibility complex class I by human ubiquitin ligases related to viral immune evasion proteins. J Virol 78: 1109–1120.
13. Ohmura-Hoshino M, Matsuki Y, Aoki M, Goto E, Mito M, et al. (2006) Inhibition of MHC Class II Expression and Immune Responses by c-MIR. J Immunol 177: 341–354.
14. Ohmura-Hoshino M, Goto E, Matsuki Y, Aoki M, Mito M, et al. (2006) A novel family of membrane-bound E3 ubiquitin ligases. J Biochem (Tokyo) 140: 147–154.
15. Duncan LM, Piper S, Dodd RB, Saville MK, Sanderson CM, et al. (2006) Lysine-63-linked ubiquitination is required for endolysosomal degradation of class I molecules. Embo J 25: 1635–1645.
16. Soubeyran P, Kowanetz K, Szymkiewicz I, Langdon WY, Dikic I (2002) Cbl-CIN85-endophilin complex mediates ligand-induced downregulation of EGF receptors. Nature 416: 183–187.
17. Levkowitz G, Waterman H, Zamir E, Kam Z, Oved S, et al. (1998) c-Cbl/Sli-1 regulates endocytic sorting and ubiquitination of the epidermal growth factor receptor. Genes Dev 12: 3663–3674.
18. Levkowitz G, Waterman H, Ettenberg SA, Katz M, Tsygankov AY, et al. (1999) Ubiquitin ligase activity and tyrosine phosphorylation underlie suppression of growth factor signaling by c-Cbl/Sli-1. Mol Cell 4: 1029–1040.
19. Kamsteeg EJ, Hendriks G, Boone M, Konings IB, Oorschot V, et al. (2006) Short-chain ubiquitination mediates the regulated endocytosis of the aquaporin-2 water channel. Proc Natl Acad Sci U S A 103: 18344–18349.
20. Zhou R, Patel SV, Snyder PM (2007) Nedd4-2 catalyzes ubiquitination and degradation of cell surface ENaC. J Biol Chem 282: 20207–20212.
21. Barriere H, Nemes C, Lechardeur D, Khan-Mohammad M, Fruh K, et al. (2006) Molecular basis of oligoubiquitin-dependent internalization of membrane proteins in mammalian cells. Traffic 7: 282–297.

22. Lehner PJ, Hoer S, Dodd R, Duncan LM (2005) Downregulation of cell surface receptors by the K3 family of viral and cellular ubiquitin E3 ligases. Immunol Rev 207: 112–125.
23. Ishido S, Wang C, Lee BS, Cohen GB, Jung JU (2000) Downregulation of major histocompatibility complex class I molecules by Kaposi's sarcoma-associated herpesvirus K3 and K5 proteins. J Virol 74: 5300–5309.
24. Coscoy L, Ganem D (2000) Kaposi's sarcoma-associated herpesvirus encodes two proteins that block cell surface display of MHC class I chains by enhancing their endocytosis. Proc Natl Acad Sci USA 97: 8051–8056.
25. Stevenson PG, Efstathiou S, Doherty PC, Lehner PJ (2000) Inhibition of MHC class I-restricted antigen presentation by gamma 2-herpesviruses. Proc Natl Acad Sci U S A 97: 8455–8460.
26. Sanchez DJ, Coscoy L, Ganem D (2002) Functional organization of MIR2, a novel viral regulator of selective endocytosis. J Biol Chem 277: 6124–6130.
27. Matsuki Y, Ohmura-Hoshino M, Goto E, Aoki M, Mito-Yoshida M, et al. (2007) Novel regulation of MHC class II function in B cells. Embo J 26: 846–854.
28. Hewitt EW, Duncan L, Mufti D, Baker J, Stevenson PG, et al. (2002) Ubiquitylation of MHC class I by the K3 viral protein signals internalization and TSG101-dependent degradation. Embo J 21: 2418–2429.
29. Matsumoto S, Miyagishi M, Taira K (2007) Genome-wide screening by using small-interfering RNA expression libraries. Methods Mol Biol 360: 131–142.

BMC Biotechnology

BioMed Central

Research article

Open Access

# Knockdown of the bovine prion gene PRNP by RNA interference (RNAi) technology

Shizuyo Sutou*[1], Miho Kunishi[1], Toshiyuki Kudo[1], Pimprapar Wongsrikeao[2,3], Makoto Miyagishi[4] and Takeshige Otoi[2]

Address: [1]School of Pharmacy, Shujitsu University, 1-6-1 Nishigawara, Okayama 703-8516, Japan, [2]Laboratory of Animal Reproduction and Biotechnology, Veterinary Sciences Yamaguch University, 1677-1 Yoshida, Yamaguchi, 753-8515, Japan, [3]Department of Surgery and Theriogenology, Faculty of Veterinary Medicine, Khonkaen University, 40000, Thailand and [4]21st Century Center of Excellence Program, Graduate School of Medicine, The University of Tokyo, Hongo 7-3-1, Bunkyo-ku, Tokyo 113-8655, Japan

Email: Shizuyo Sutou* - sutou@shujitsu.ac.jp; Miho Kunishi - kunishi@shujitsu.ac.jp; Toshiyuki Kudo - kudo@shujitsu.ac.jp; Pimprapar Wongsrikeao - Pimprapar@yahoo.com; Makoto Miyagishi - makoto-m@sannet.ne.jp; Takeshige Otoi - otoi@yamaguchi-u.ac.jp

* Corresponding author

Published: 26 July 2007

*BMC Biotechnology* 2007, **7**:44 doi:10.1186/1472-6750-7-44

Received: 12 November 2006
Accepted: 26 July 2007

This article is available from: http://www.biomedcentral.com/1472-6750/7/44



## Abstract

**Background:** Since prion gene-knockout mice do not contract prion diseases and animals in which production of prion protein (PrP) is reduced by half are resistant to the disease, we hypothesized that bovine animals with reduced PrP would be tolerant to BSE. Hence, attempts were made to produce bovine *PRNP* (b*PRNP*) that could be knocked down by RNA interference (RNAi) technology. Before an in vivo study, optimal conditions for knocking down b*PRNP* were determined in cultured mammalian cell systems. Factors examined included siRNA (short interfering RNA) expression plasmid vectors, target sites of *PRNP*, and lengths of siRNAs.

**Results:** Four siRNA expression plasmid vectors were used: three harboring different cloning sites were driven by the human U6 promoter (hU6), and one by the human $tRNA^{Val}$ promoter. Six target sites of bovine *PRNP* were designed using an algorithm. From 1 (22 mer) to 9 (19, 20, 21, 22, 23, 24, 25, 27, and 29 mer) siRNA expression vectors were constructed for each target site. As targets of siRNA, the entire b*PRNP* coding sequence was connected to the reporter gene of the fluorescent EGFP, or of firefly luciferase or *Renilla* luciferase. Target plasmid DNA was co-transfected with siRNA expression vector DNA into HeLaS3 cells, and fluorescence or luminescence was measured. The activities of siRNAs varied widely depending on the target sites, length of the siRNAs, and vectors used. Longer siRNAs were less effective, and 19 mer or 21 mer was generally optimal. Although 21 mer GGGGAGAACTTCACCGAAACT expressed by a hU6-driven plasmid with a *Bsp* MI cloning site was best under the present experimental conditions, the corresponding tRNA promoter-driven plasmid was almost equally useful. The effectiveness of this siRNA was confirmed by immunostaining and Western blotting.

**Conclusion:** Four siRNA expression plasmid vectors, six target sites of b*PRNP*, and various lengths of siRNAs from 19 mer to 29 mer were examined to establish optimal conditions for knocking down of b*PRNP* in vitro. The most effective siRNA so far tested was 21 mer GGGGAGAACTTCACCGAAACT driven either by a hU6 or tRNA promoter, a finding that provides a basis for further studies in vivo.

## Background

Prion diseases are characterized by a prolonged latent period and a distinctive neuropathology that includes spongiform change, gliosis, neuronal loss, and the accumulation of an abnormal prion protein ($PrP^{Sc}$), an isomer of the normal cellular prion protein ($PrP^{C}$) encoded by the prion gene (*PRNP*), in affected brains. $PrP^{C}$, a glycoprotein, is anchored to the outer surface of neurons and to a lesser extent of lymphocytes and other cells. The function of $PrP^{C}$ is not known, but seems to be physiologically important because *PRNP* has been found in all animals examined (cattle, goats, hamsters, humans, mice, rats, sheep) as well as in the chicken. The conversion of $PrP^{C}$ to $PrP^{Sc}$ is believed to occur not as a result of viral or bacterial infection but as a result of interaction with exogenously introduced, self-replicating $PrP^{Sc}$ or by a very rare spontaneous event according to the protein-only hypothesis [1].

Although data have been accumulated using BSE-infected mice [2] and *Prnp* knockout mice as well [3-5], the physiological role of $PrP^{C}$ still remains to be clarified. From the pathological viewpoint, however, it is important that mice devoid of $PrP^{C}$ are resistant to scrapie and fail to propagate prions [6-9] and that the introduction of PrP-encoding transgenes restores susceptibility to the disease [10]. *Prnp*0/+ mice, which have about half the normal level of $PrP^{C}$ in their brains, show enhanced resistance to scrapie, as revealed by a significant delay in the onset and progression of clinical disease, while in wild-type animals, an increase in prion titer and $PrP^{Sc}$ levels was followed within weeks by symptoms of scrapie and death [11]. These findings suggest that the production of BSE-resistant cattle would be possible by knocking down bovine *PRNP* (b*PRNP*) using RNA interference (RNAi) technology.

The injection of double-stranded RNA (dsRNA) into the cells of worms led to efficient sequence-specific gene silencing, referred to as RNAi [12]. This phenomenon also occurs in fly and plant cells, but not in mammalian cells. However, Elbashir et al. [13] demonstrated that 21~22-nt dsRNA with 2-nt 3' overhangs (short interfering RNA: siRNA) can induce sequence-specific gene silencing without non-specific inhibition of gene expression in cultured mammalian cells. siRNA expression systems using plasmid vectors are advantageous, because their use makes it possible to make transgenic animals, and the incorporation of one or a few plasmids into the nucleus would provide enough siRNA to induce RNAi. Soon after the discovery by Elbashir et al. [13] of the occurrence of RNAi in mammals, siRNA expression vector systems were developed [14-16]. The current understanding of the mechanisms of RNAi is as follows: dsRNA is digested to siRNA by the actions of Dicer, a family member of RNase III enzymes [17], and one strand of the siRNA unwound with the aid of ATP hydrolysis is incorporated into RISC (RNA-induced silencing complex) which has RNase activity [18]. mRNA with the sequence complementary to the siRNA is cleaved by RISC, knocking-down the gene expression of a specified mRNA (Dykxhoom et al., review [19]). Here we present optimal conditions, including siRNA expression promoters, target sites, and lengths of siRNAs, for knocking down b*PRNP*.

## Results

### *Target plasmids with the insertion of a stop codon between reporter and target genes*

In previous experiments, a full-length mouse *Prnp* gene with ATG (762 bp) or without ATG (759 bp) and three other fragments (645, 486, and 306 bp from the stop codon) were ligated in-frame into pDsRed2-C1. Cells transfected with the full-length construct and the plasmid with the 486-bp fragment did not show fluorescence, but cells transfected with the plasmids containing the 645-bp and 306-bp fragments emitted fluorescence, indicating that in-frame inserts might stop the production of the fluorescent reporter depending on the sequence. When the full-length b*PRNP* was inserted into pEGFP-C1 downstream from the EGFP stop codon, cells transfected with the construct emitted fluorescence. Therefore, a stop codon was inserted between the reporter and b*PRNP* in all the target plasmids, all of which were found to be effective in producing fluorescence in transfected cells (Table 1).

### *Dose-response relationship between fluorescence and plasmid DNA*

When the dose-response relationship was examined using pEGFP-bPrP, linearity of EGFP fluorescence was obtained below 500 ng/well; a total of 400 ng/well or less was therefore used in subsequent experiments.

### *Comparison of sensitivity of fluorescence versus luminescence and lengths of siRNAs*

When the sensitivity of the fluorescent reporter of pEGFP-bPrP (Fig. 1A) and the luminescent reporter of pGL3-bPrP (Fig. 1B) was compared, detection of the EGFP fluorescence was found to be less sensitive than detection of the luminescence produced by firefly luciferase. This may be due to the comparatively long life of EGFP protein. Fig. 1A also shows that shorter siRNAs (around 23 mer) were more effective in silensing b*PRNP* expression than longer ones (27 and 29 mer), and that piGENE tRNA was more effective than piGENE CACC-S/K. Fig. 1B compares a narrow range of lengths of siRNAs expressed by three plasmid vectors. On the whole, 21 or 22 mer was the most effective silencer, and the differences between them were minor.

### *Vectors harboring internal control emitters*

To determine the effectiveness of siRNAs, measurements of reporter protein levels were made using fluorescence or luminescence reporter assays (Fig. 1A and 1B). Three vec-

**Table 1: Characteristics of target vectors**

| Vector | Promoter 1 | Reporter 1 | Target | Promoter 2 | Reporter 2 | Target |
|---|---|---|---|---|---|---|
| pEGFP-bPrP | CMV | EGFP | *bPRNP* | | | |
| pGL3-bPrP | SV40 | Fire-fly luciferase | *bPRNP* | | | |
| pFluc-bPrP-Rluc | SV40 | Fire-fly luciferase | *bPRNP* | HSV-TK | Renilla luciferase* | |
| pFluc-Rluc-bPrP | SV40 | Fire-fly luciferase* | | HSV-TK | Renilla luciferase | *bPRNP* |
| pTKFluc-bPrP-Rluc | HSV-TK | Fire fly luciferase | *bPRNP* | HSV-TK | Renilla luciferase* | |

*, used as the internal control.

tors in which an internal control was integrated into a single target vector, pFluc-bPrP-Rluc, pFluc-Rluc-bPrP, and pTKFluc-bPrP-Rluc, were constructed (Table 1). Since the results obtained with pTKFluc-bPrP-Rluc were almost the same as those for pFluc-Rluc-bPrP and pTKFluc-bPrP-Rluc, the results for pFluc-bPrP-Rluc are shown in Fig. 1C, in which effective target sites are compared (see next section). *Renilla* luminescence was always much stronger than firefly luminescence driven by either the SV40 or HCV-TK promoter. Although the sensitivity of siRNA effects detected using these double emitter vectors was low compared with that of a single emitter such as pGL3-bPrP, the relative effectiveness of siRNA was reproducible. Therefore, these vectors appeared to be useful for assaying the relative activity.

### *Effective target sites*

Six siRNA target sites were predicted in the b*PRNP* sequence by using an algorithm [20] (Nos. 1, 3, 5, 6, 15 and 17, Table 2). Six different 22-nt targets (Nos. 2, 4, 5, 8, 16 and 18, Table 2), except for No. 8, where a 21 mer was used, were compared using a single expression vector, piGENE hU6 (Fig. 1C). The target vector was pFluc-bPrP-Rluc and the sensitivity was quite low, as described previously, but relative activities could be determined. No. 8 with the sequence 5'-GGGGAGAACTTCACCGAAACT-3' was the best silencer. Fig. 1D shows differences in siRNA activities examined using combinations of four target sites of 22 nt (Nos. 2, 4, 9, and 16, Table 2) and three expression vectors (piGENE CACC-S/K, piGENE S/K, and piGENE tRNA. Table 3). As for vectors, piGENE S/K was the best, followed by piGENE tRNA; and piGENE CACC-S/K was almost always the worst. As for target sites, sequence No. 9, the 22 mer version of No. 8 (21 mer), was the best and No. 4 was the worst using all three vectors. Differences between 21 mer and 22 mer were minimal in the three vectors (Fig. 1D).

### *Comparison of siRNA expression vectors*

The structure of the cloning sites of the siRNA expression vectors is shown in Table 3. Fig 1E compares the effectiveness of the siRNA expression vectors. Fig. 1E shows a typical result, and the order of effectiveness was almost always piGENE hU6, piGENE S/K, piGENE tRNA, and piGENE CACC-S/K. The difference between piGENE hU6 and piGENE S/K was minimal and sometimes the order of these two was reversed.

### ***bPRNP* silencing as revealed by immunostaining**

Full-length $PrP^C$ and truncated $PrP^C$ as targets and three antibodies, SAF32, P6488, and anti-FLAG, recognizing different regions, the upstream, mid-part, and C-terminal tag, respectively, were used for immunostaining experiments. Full-length $PrP^C$ could be detected equally using the three antibodies; the fluorescence signal intensities, which were moderate, were almost the same (Fig. 2A and 2C) among the three. The number of fluorescent cells depended on the amount of target DNA applied. When 800 ng/well was applied, approximately 50% of cells were fluorescence-positive, and when 200 ng/well was used, 20–30% were positive. When target DNA was co-transfected with siRNA expression vector DNA, almost no fluorescence was detected (Fig. 2B). This was true for both hU6 and tRNA promoter-driven vectors (Fig. 2B and 2D). Truncated $PrP^C$ could be detected using P6488 (Fig. 2E) and anti-FLAG antibody. As expected, SAF32 could not detect truncated $PrP^C$, which lacks the N-terminal region (not shown). The intensity of fluorescence was much stronger than that of full-length $PrP^C$ (compare Fig. 2E with A and C). Perinuclear regions were strongly stained (Fig. 2E). The fluorescence almost disappeared when target DNA was co-transfected with siRNA expression plasmid DNA derived from either piGENE hU6 (Fig. 2F) or piGENE tRNA, indicating the effectiveness of siRNA.

### ***bPRNP* silencing as revealed by Western blotting**

When a full-length $PrP^C$ was transiently expressed and detected using the antibody SAF32, 25- to 30-kDa bands were detected, with the 26-kDa band being most intense. When target DNA was co-transfected with siRNA expression vector DNA, almost no bands were detected (Fig 3), indicating the effectiveness of siRNA. This was true for both hU6 (Fig 3, lanes 8–10) and tRNA (Fig 3, lanes14–16) promoter-driven vectors. The bands in lanes 5–7 were darker than those in lanes 11–13. Sonication of the samples in lanes 11–13 seemed to have been insufficient, because intense bands were seen at the sites of sample application. The major band was 26 kDa, non-glyco-

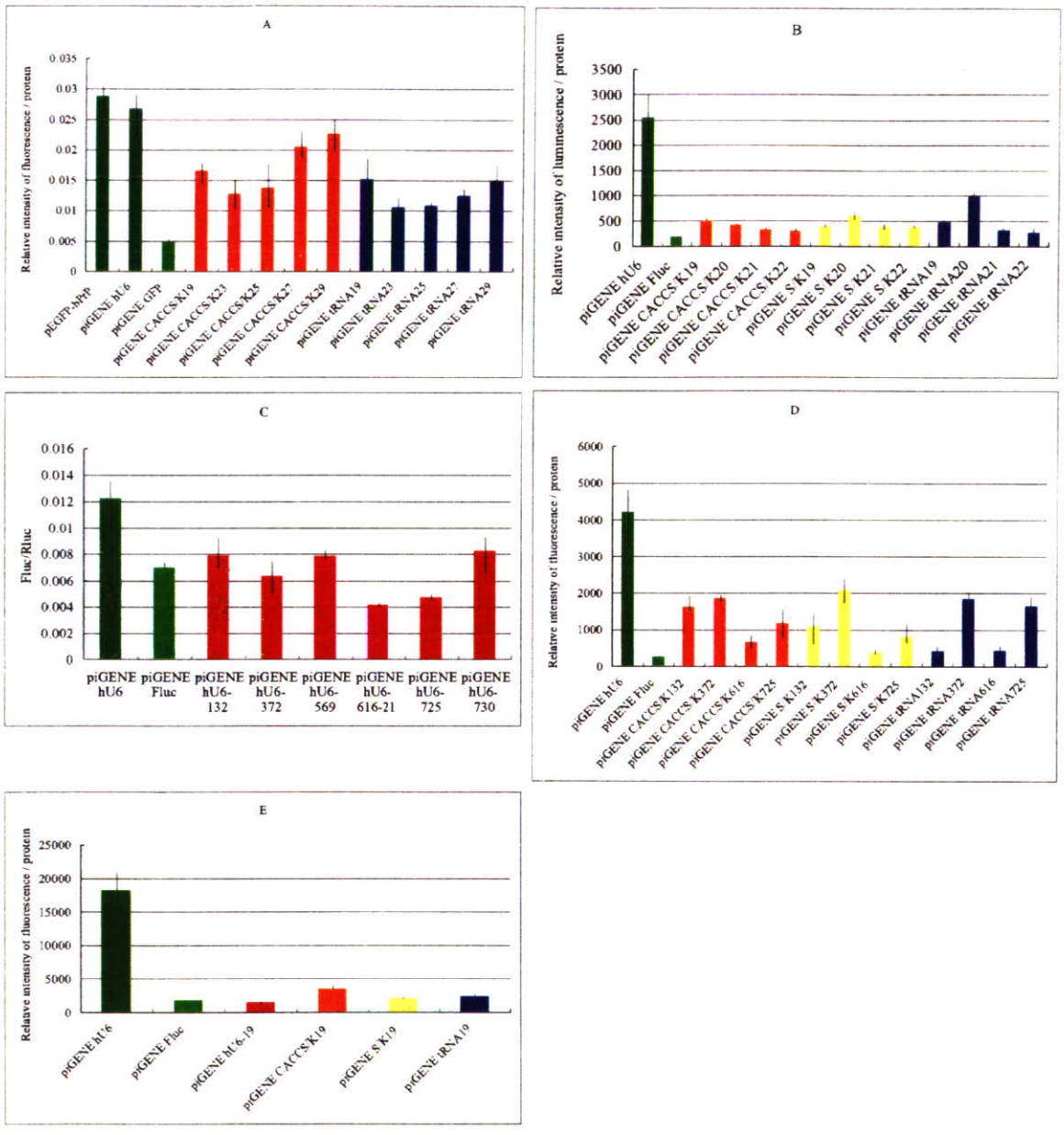


**Figure 1**

**Effects of siRNA expression vectors on b*PRNP***. A and B, effects of different lengths of siRNAs expressed by different vectors. A: piGENE hU6-EGFP was a positive control siRNA vector for EGFP. Numerals after vectors indicate the lengths of siRNA; 19, 23, 25, 27, and 29 correspond to No. 6, 10, 12, 13, and 14 in Table 2, respectively. B: piGENE Fluc is a positive control siRNA vector against firefly luciferase. Numerals after vectors indicate the lengths of siRNA; 19, 20, 21, and 22 correspond to No. 6, 7, 8, and 9 in Table 2, respectively. C and D, effects of different target sites and expression vectors on siRNA activities. C: numerals after vectors indicate the start sites of siRNA; 132, 372, 616, and 725 correspond to No. 2, 4, 9, and 16 in Table 2, respectively. D: as for numerals after vectors, see the legend to C. E: comparison of vector activities. Vectors expressed 19 mer, and the sequence corresponds to No. 6 in Table 2.

**Table 2: Target sequences examined**

| No. | Position[a] | sequence | nt | Constructed vectors (○)[b] | | | | Value[c] |
|---|---|---|---|---|---|---|---|---|
| | | | | hU6 | CACC-S/K | S/K | tRNA | |
| 1 | 132–150 | GGGCAGTCCTGGAGGCAAC | 19 | ○ | ○ | ○ | ○ | 0.779 |
| 2 | 132–153 | GGGCAGTCCTGGAGGCAACCGT | 22 | ○ | ○ | ○ | ○ | |
| 3 | 372–390 | AGGAGCTGCTGCAGCTGGA | 19 | ○ | ○ | ○ | ○ | 0.775 |
| 4 | 372–393 | AGGAGCTGCTGCAGCTGGAGCA | 22 | ○ | ○ | ○ | ○ | |
| 5 | 569–591 | GTGTCAATATCACAGTCAAGGA | 22 | ○ | | | | 0.757 |
| 6 | 616–634 | GGGGAGAACTTCACCGAAA | 19 | ○ | ○ | ○ | ○ | 0.852 |
| 7 | 616–635 | GGGGAGAACTTCACCGAAAC | 20 | ○ | ○ | ○ | ○ | |
| 8 | 616–636 | GGGGAGAACTTCACCGAAACT | 21 | ○ | ○ | ○ | ○ | |
| 9 | 616–637 | GGGGAGAACTTCACCGAAACTG | 22 | ○ | ○ | ○ | ○ | |
| 10 | 616–634 | GGGGAGAACTTCACCGAAACTGA | 23 | ○ | ○ | ○ | ○ | |
| 11 | 616–634 | GGGGAGAACTTCACCGAAACTGAT | 24 | ○ | | | | |
| 12 | 616–634 | GGGGAGAACTTCACCGAAACTGACA | 25 | ○ | ○ | ○ | ○ | |
| 13 | 616–634 | GGGGAGAACTTCACCGAAACTGACATC | 27 | ○ | ○ | ○ | ○ | |
| 14 | 616–634 | GGGGAGAACTTCACCGAAACTGACATCAA | 29 | ○ | ○ | ○ | ○ | |
| 15 | 725–743 | GTGTGATCCTCTTCTCTTC | 19 | ○ | ○ | ○ | ○ | 0.772 |
| 16 | 725–746 | GTGTGATCCTCTTCTCTTCCCC | 22 | ○ | ○ | ○ | ○ | |
| 17 | 730–748 | ATCCTCTTCTCTTCCCCTC | 19 | ○ | | | | 0.752 |
| 18 | 730–751 | ATCCTCTTCTCTTCCCCTCCTG | 22 | ○ | | | | |

a, Position 1 starts from A of ATG, the first codon of b*PRNP*. b, hU6, CC-S/K, S/K, and tRNA indicate piGENE hU6, piGENE CACC-S/K, piGENE S/K, and piGENE tRNA, respectively (Table 3). Open circles designate construction of vectors. c, Values were obtained from the prediction algorithm [20].

sylated $PrP^C$. Glycosylated $PrP^C$ appeared at around 32 kDa, as can be clearly seen in lanes 5–7, and very faintly seen in lanes 11–13. The nature of the strong bands at around 40 kDa in lanes 5–7 is not known. Truncated $PrP^C$ could not be detected using SAF32, as expected, but could be detected using P6488 antibody (data not shown).

## Discussion

The hU6 promoter has been widely used to drive siRNA expression in plasmid vectors, but tRNA promoter-driven vectors have rarely been used; therefore, in this study piGENE tRNA was used for comparison with piGENE hU6. These two vectors have different cloning sites, i.e., piGENE hU6 has a *Bsp* MI cloning site, while the piGENE tRNA has a *Sac* I, *Bgl* II, *Not* I, *Kpn* I, and *Eco* RV cloning site, (Table 3). The instructions of the manufacturer are also different: 19 to 22 mer is reccomended for piGENE hU6 and less than or close to 30 mer for piGENE tRNA. siRNA activities are affected by the promoters, siRNA lengths, and cloning site structures. To compare the effectiveness of piGENE hU6 and piGENE tRNA, two other siRNA-expression vectors were constructed; these were piGENE CACC-S/K and piGENE S/K, which had a common cloning site consisting of *Sac* I, *Bgl* II, *Eco* RV, and *Kpn* I recognition sequences. Using the *Sac* I and *Kpn* I sites was convenient because the same constructs could be employed as cassettes for piGENE CACC-S/K, piGENE S/K, and piGENE tRNA (Table 3). CACC was introduced into piGENE CACC-S/K because the natural human U6 promoter habors a G just after CACC, which enhances transcription [20].

siRNA activities can depend on the target genes and their sequences, and therefore definite and universal conclusions cannot be made. However, the present data indicate that a shorter siRNA (around 19 to 22 mer rather than 30 mer) is better for piGENE tRNA. As a whole, piGENE hU6 showed higher levels of siRNA expression activity than piGENE tRNA. piGENE hU6 and piGENE S/K had almost the same levels of activity, but the former seemed to be slightly better. The *Sac* I recognition site is GAGCTC and the insertion of DNA for siRNA expression occurred just after this site. On the other hand, the inserts come after CACCGAGCTC in piGENE CACC-S/K, the siRNA transcription of which might start from G, A, or G in the *Sac* I recognition site, and Dicer counts base numbers from these starting sites. An unexpected early start to transcription would leave several bases at the 3' end behind and lead to a shortage of matching bases to target mRNAs, lessening siRNA acrtivity.

As for the length of siRNA, 22 mer was generally the best (Fig. 1B), although 21 mer sometimes showed similar or better activity. However, 20 mer usually showed less activ-

**Table 3: Structure of cloning sites of siRNA expression vectors**

| Vector | Promoter | Sequence of cloning site |
|---|---|---|
| piGENE hU6 | hU6 | CACCGTGAGCAGGTGTAAAGCCACCATGGAAGACACCTGCCAAC<br>*TTTTTT*CAATTGGTCGACCTGCAGGCATGCAAGCTT[a] |
| piGENE CACC-S/K | hU6 | CACCGAGCTCAGACTCGATATCGGTACC[b] |
| piGENE S/K | hU6 | GAGCTCAGACTCGATATCGGTACC[c] |
| piGENE tRNA | tRNA | GAGCTCCAGATCTAATGCGGCCGCTTAGGTACCATAGATATC*TTTTTTT*CTGCAGGCATGCAAGCTT[d] |

a: Three *Bsp* MI sites are underlined. b and c: *Sac* I, *Bgl* II, *Eco* RV, and *Kpn* I sites are underlined. d: *Sac* I, *Bgl* II, *Not* I, *Kpn* I, *Eco* RV, *Pst* I, and *Hind* III sites are underlined. T repeats, RNA pol III terminator signal, are italicized.

ity than 19 mer, 21 mer or 22 mer (Fig. 1B). The reasons for this are not known, but Dicer's mechanisms of action might be involved.

The target sequence No. 6, 5'-GGGGAGAACTTCACCGAAA-3', achieved the highest score among the six targets (Table 2). Principles for the prediction of a favorable siRNA have been proposed [21,22]. One of the key factors in RNAi is the assembly of RISC, which mediates target RNA cleavage. The sense and anti-sense strands of an siRNA duplex are not equally eligible for assembly into RISC. Both the absolute stability and relative stability of the base pairs at the 5' end of siRNA seem to determine which strand takes part in the RNAi pathway. Given that in the conventional way of writing DNA sequences, the sense strand is the upper one and the anti-sense strand is the lower one, the left end should be tight and the right end should be loose for the anti-sense strand to be incorporated into RISC. In such an analysis, No. 6 has a tight left and a loose right end, and thus it is theoretically predicted to be effective, and was in fact found to be effective. This tightness and looseness do not always determine the effectiveness of RNAi, but are important factors.

The purpose of the present study was to knockdown b*PRNP* using RNAi technology. We used, however, an siRNA expression vector driven by a hU6 promoter and human HeLaS3 cells in an in vitro system. Is the hU6 promoter active in bovine cells? Recently, we [23] cloned chicken U6 promoters and examined their activity in chick cells using the hU6 promoter as a comparative control. Chicken and human promoters showed almost the same level of activity, although the activity levels were not very high. Lambeth et al. [24] cloned a bovine U6 promoter and examined its activity in MDBK (Madin Darby Bovine Kidney) and Vero (African Green monkey kidney) cells together with the mouse U6 promoter. The U6s of both species gave almost identical results, suggesting that the hU6 promoter might also be active in different mammalian cells. Indeed, our experiments showed that siRNA driven by hU6 was active in bovine primary cultured cells (data not shown).

## Conclusion

To produce b*PRNP*-knocked down cattle using RNA interference (RNAi) technology, optimal conditions for knocking down were first investigated in vitro. Four siRNA expression plasmid vectors, six target sites of b*PRNP*, and various lengths of siRNA from 19 mer to 29 mer were examined. As a target, the b*PRNP* coding sequence was connected to the reporter of the fluorescent EGFP, firefly luciferase, or *Renilla* luciferase gene. When target plasmid DNA was co-transfected with siRNA expression vector DNA into HeLaS3 cells, and fluorescence or luminescence was measured, siRNA of 21 mer GGGGAGAACTTCACCGAAACT expressed by a hU6- or tRNA-driven plasmid gave the best knockdown result under the present experimental conditions. The effectiveness of this siRNA was confirmed by immunostaining and Western blotting. These data provide a basis for further studies in vivo.

## Methods

### *Cloning of bovine prion gene* PRNP

b*PRNP* consists of three exons, with the open reading frame (ORF) being located in exon 3 [25,26] (see also GeneBank Accession No. D10612). An ORF consisting of 792 bp encoding 264 amino acid residues was amplified by PCR with a pair of primers, one with a *Bgl* II site at the terminus and the other with a *Hind* III site. The PCR product was inserted into a TOPO vector (Invitrogen, Carlsbad, CA).

### PRNP *target vectors*

pEGFP-C1, which harbors a green fluorescent protein gene driven by the CMV promoter, was purchased from Becton, Dickinson and Company, Japan (Tokyo, Japan). The multiple cloning sites of the vector were changed to *Bsr* GI-*Bsp* EI-*Spe* I-*Bgl* II-*Sal* I-*Afl* II-*Spl* I-*Cla* I-*Apa* I-*Sma* I/*Xma* I-*Bam* I-*Xba* I-*Bcl* I. This vector has an in-frame stop codon, TAG, in the *Spe* I recognition site (ACTAGT), which deletes the translation of inserts cloned downstream of the *Bgl* II site so as not to interfere with the intensity of fluorescence. pGL3 control and pRL-TK, which harbor the firefly luciferase gene (Fluc) driven by the SV40 promoter and the *Renilla* luciferase gene (Rluc)